REVIEW ARTICLE

Miocene vegetation and climate in the eastern North Sea Basin, onshore Denmark, compared to the present

Kasia K. Śliwińska*[1] , Thomas Denk[2] , Karen Dybkjær[1] , Julie Margrethe Fredborg[3] , Sofie Lindström[3,4] , Stefan Piasecki[5,6] , Erik Skovbjerg Rasmussen[6]

[1]Department of Geo-energy and Storage, Geological Survey of Denmark and Greenland (GEUS), Copenhagen, Denmark; [2]Swedish Museum of Natural History, Stockholm, Sweden; [3]Department of Geosciences and Natural Resource Management, University of Copenhagen, Copenhagen, Denmark; [4]Geological Survey of Denmark and Greenland (GEUS), Copenhagen, Denmark; [5]Globe Institute, University of Copenhagen, Copenhagen, Denmark; [6]Department of Geophysics and Sedimentary Basins, Geological Survey of Denmark and Greenland (GEUS), Copenhagen, Denmark

Abstract

Despite often being referred to as a 'coolhouse climate', the climate during the Miocene (23.03–5.33 Ma) was overall humid, warm and temperate. It was paced by orbitally driven cooler periods (the Oligocene–Miocene Transition and Mi-events) overprinted by a climatic optimum. Global cooling during the Late Miocene brought more arid conditions with climate seasonality, which varied across western Eurasia. Sedimentary archives from onshore Denmark comprise shallow marine siliciclastic deposits and discrete brown coal layers. Hence, they allow us to infer past climates and environments using both marine and terrestrial fossils. The backbone for Miocene stratigraphy and palaeoclimate reconstruction in the eastern North Sea Basin (present-day Denmark) is the Sønder (Sdr.) Vium sediment core, which penetrates a shallow marine succession and spans an interval from c. 22 to 8 Ma. Here, we present an improved age model for the core. During the Miocene, forested lowlands predominated in the eastern North Sea Basin. Coastal areas included rich riparian landscapes and delta areas of lignite-forming swamp forest. Compilations of existing proxy records (pollen, spores, leaves, plant fragments and the organic biomarkers alkenones and membrane lipids) collectively show that the climate here was warm and moist during the Early and Middle Miocene, while the Late Miocene was characterised by climate cooling and modernisation of the vegetation. The interval preceding the Miocene Climatic Optimum was already warm and moist, and the onset was not characterised by a significant increase in temperature and precipitation. Instead, the palynoflora indicates homogeneous vegetation and only a weak signal of warming shown by a minor increase of, for example, sabaloid palms and Mastixiaceae.

1 Introduction

The Miocene (23.03–5.33 Ma) witnessed the final transition from the 'coolhouse' climate of the Oligocene (with a permanent ice sheet covering Antarctica) to the modern 'icehouse' world characterised by bipolar glaciation. The coolhouse climate commenced c. 34 Ma and the transition from the preceding 'greenhouse' climate was driven by a decline in atmospheric CO_2 and changes in ocean gateways and current systems (Stickley *et al.* 2004; Pearson *et al.* 2009; Cristini *et al.* 2012; Anagnostou *et al.* 2016; Hutchinson *et al.* 2019). During the Oligocene (34–23.03 Ma), atmospheric CO_2 may have decreased to values as low as 400 ppm (Rae *et al.* 2021) and several orbitally paced glaciations occurred in Antarctica (Wade & Pälike 2004; Pälike *et al.* 2006). In the North Atlantic – North Sea – Nordic Seas region, some of these events show a strong correlation with episodes of cooling of surface waters and decreasing sea levels (Śliwińska *et al.* 2010; Śliwińska & Heilmann-Clausen 2011; Clausen *et al.* 2012; Śliwińska 2019).

One of the major glaciations and cooling events of the coolhouse world took place during the Oligocene–Miocene Transition (OMT), where global cooling coincided with a drop in sea level (Miller *et al.* 2005) marked by a

transient, large amplitude expansion of Antarctic ice sheets. The associated glacial maximum is expressed by a positive shift of *c.* 1‰ in stable oxygen-isotope values (δ^{18}O) measured in benthic foraminifera. This shift was one of the largest, abrupt (<1 Myr) increases in benthic δ^{18}O observed for the Cenozoic (Lear *et al.* 2004). The occurrence of orbitally paced transient glacial episodes continued during the Miocene (e.g. Miller *et al.* 1991; Miller & Mountain 1996). However, in the eastern North Sea Basin (present-day Denmark), glacioeustatic sea-level fluctuations were superimposed on tectonically driven sea-level changes, making it difficult to decouple these two factors (Rasmussen 2004).

Although the Miocene was significantly cooler than the previous epochs of the Cenozoic, the climate was relatively warmer and wetter than today; hence, it is more appropriately referred to as coolhouse than icehouse (Westerhold *et al.* 2020). Atmospheric CO_2 in the Miocene and the following Pliocene might have reached 200–400 ppm (The Cenozoic CO_2 Proxy Integration Project (CenCO$_2$PIP) Consortium 2023). The type of coolhouse climate known from *c.* 34 to 3.5 Ma (Westerhold *et al.* 2020) was interrupted by an interval of transient warmth, known as the Miocene Climatic Optimum (MCO) *c.* 16.9–14.7 Ma (e.g. Shackleton & Kennett 1975; Zachos *et al.* 2001). The MCO was the warmest period over the last 23 Myr (Zachos *et al.* 2001) associated with a minimum ice volume in Antarctica (Holbourn *et al.* 2007). The warming was caused by elevated atmospheric CO_2, most possibly caused by intense volcanism primarily from the Columbia River Basalts eruptions (e.g. Kasbohm & Schoene 2018). The MCO was the last time in Earth's history where atmospheric CO_2 was as high as it is today, and possibly higher at *c.* 500 ppm (The Cenozoic CO_2 Proxy Integration Project (CenCO$_2$PIP) Consortium 2023). With atmospheric CO_2 > 420 ppm and global mean temperatures *c.* 7–8°C warmer than present, the MCO falls in the middle range of climate states predicted for Representative Concentration Pathway (RCP) 4.5 and RCP 6.0 (Collins *et al.* 2013; where 4.5 and 6.0 are the stabilised levels of radiative forcing expected by 2100 according to different emission scenarios). Therefore, the MCO is considered one of the most accurate reference intervals for a possible future climate. Up to 3°C of the warming observed in the Middle (Goldner *et al.* 2014) and Late Miocene (Knorr *et al.* 2011) can be explained by the differences in palaeo-oceanography (continent position, seaways and ocean current systems), topography and vegetation when compared with the modern state. The remaining temperature increase of the MCO is attributed to elevated atmospheric CO_2 clearly showing its strong impact on the global climate.

Today, atmospheric CO_2 has already surpassed 400 ppm, and so mid-Pliocene warming at 400 ppm CO_2 is considered an optimistic 'best-case scenario' for the near-future. In this scenario, Earth's anthropogenic global temperature anomaly by 2100 is limited to 1.5–2°C (Schellnhuber *et al.* 2016) above pre-industrial times. With atmospheric CO_2 >450 ppm, elevated global temperatures and a more intense hydrological cycle, the MCO is often considered the most recent climatic optimum in Earth's history that is comparable with today's climate. Thus, following a moderate CO_2 emission scenario, it may be more realistic that we reach a similar climatic condition as the MCO by 2100.

Despite being more critical for our understanding of tipping points in the global climate system under CO_2 emission scenarios >450 ppm, the transition towards the MCO is poorly studied, and most existing studies of proxy records focus on the maximum. In contrast to the well-studied Antarctic ice sheet, the existence and potential extent of the Greenland ice sheet at the MCO is highly uncertain (Thiede *et al.* 2010). In Europe, the only long-term palaeotemperature record across the Middle Miocene transition north of 55°N is from Denmark.

The MCO was followed by a period of a major growth of the East Antarctic ice sheet and an associated cooling, termed the Middle Miocene Climate Transition (MMCT; 14.7–13.8 Ma; Flower & Kennett 1994). The MMCT was associated with large changes in the global carbon cycle and in the terrestrial biosphere, including aridification of midlatitude continental regions (e.g. Flower & Kennett 1994). Increased stability of the Antarctic ice sheet after 14.8 Ma represents a crucial step in the establishment of the near-modern climate system. Sea-surface temperature (SST) reached near-modern values 7–5.4 Ma (Herbert *et al.* 2016). The late Miocene cooling led to the development of C4 grasslands (Cerling *et al.* 1993). These large-scale climate-driven shifts in vegetation and landscape led to major turnovers in the terrestrial fauna favouring browsers feeding on grasses and shrubs (e.g. Badgley *et al.* 2008). Changes in terrestrial animal and plant communities together with drier conditions across large areas of the continents gave rise to a world that is similar to that we know today.

In this review, we provide an overview of the state-of-the-art knowledge regarding Miocene palaeogeography, vegetation and climatic conditions for the eastern North Sea Basin based on data from onshore Denmark. This is followed by a comparison of Miocene climate conditions with those of the present day for the wider North Atlantic region.
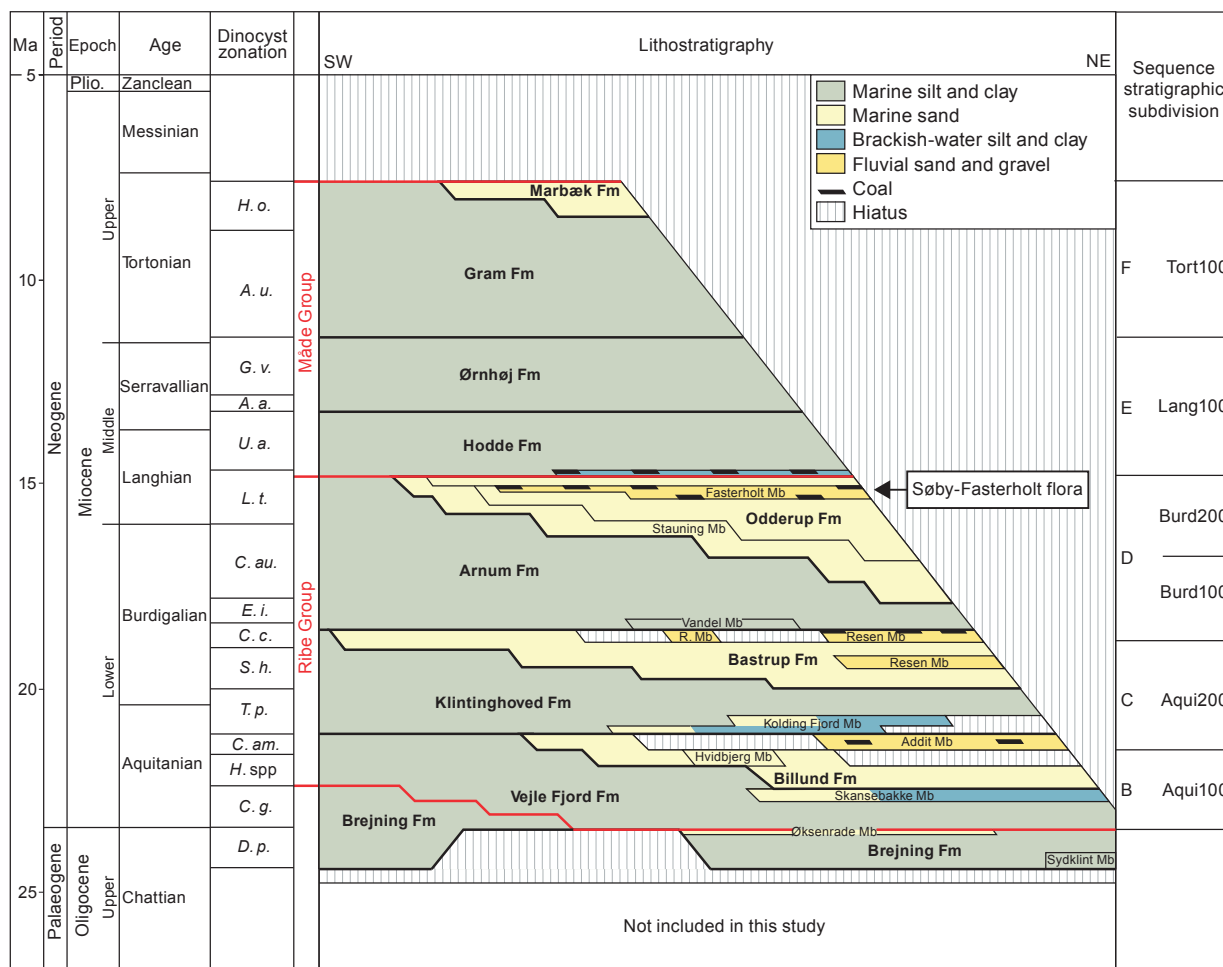
Fig. 1 Lithostratigraphic framework of the uppermost Oligocene–Miocene onshore Denmark (modified from Rasmussen *et al.* 2010). **Plio.**: Pliocene. **R. Mb**: Resen Mb. **H. o.**: *Hystrichosphaeropsis obscura*. **A.u.**: *Amiculosphaera umbracula*. **G. v.**: *Gramocysta verricula*. **A. a.**: *Achomosphaera andalousiense*. **U. a.**: *Unipontidinium aquaeductum*. **L. t.**: *Labyrinthodinium truncatum*. **C. au.**: *Cousteaudinium aubryae*. **E. i.**: *Exochosphaeridium insigne*. **C. c.**: *Cordosphaeridium cantharellus*. **S. h.**: *Sumatradinium hamulatum*. **T. p.**: *Thalassiphora pelagica*. **C. am.**: *Caligodinium amiculum*. **H. spp.**: *Homotryblium* spp. **C. g.**: *Chiropteridium galea*. **D. p.**: *Deflandrea phosphoritica*.

2 Danish Miocene stratigraphy and the Sønder (Sdr.) Vium core

The total composite thickness of the Miocene deposits onshore Denmark is *c.* 250 m, reaching up to 400 m in local depressions. The deposits consist mainly of clay, silt and sand. The succession is subdivided into the Brejning Fm (partially upper Oligocene), Vejle Fjord Fm, Klintinghoved Fm, Bastrup Fm, Arnum Fm, Odderup Fm, Hodde Fm, Ørnhøj Fm, Gram Fm and Marbæk Fm (Fig. 1). The succession is predominantly marine (outer to inner neritic), interfingered by fluviodeltaic deposits. Each of the fluviodeltaic sequences terminates with a brown coal layer (see Section 3.3 for a description).

The Danish Miocene succession is unconformably overlain by Holocene deposits. In present-day onshore Denmark, the youngest Miocene strata are of Tortonian age (Dybkjær & Piasecki 2010; Rasmussen *et al.* 2010). The succession is well dated using dinoflagellate cysts (i.e. dinocysts; Piasecki 1980; Dybkjær 2004;

Dybkjær & Piasecki 2010; Rasmussen *et al.* 2010). A few studies have provided dinocyst stratigraphy integrated with other microfossil groups, such as foraminifera (Miller *et al.* 1991; Dybkjær & Piasecki 2010; Anthonissen 2012; King *et al.* 2016), but a complete, integrated stratigraphy for the entire Danish Miocene succession does not yet exist. Furthermore, calcareous benthic foraminifera do not occur continuously throughout the Miocene succession onshore Denmark, and studies are limited to assemblage analysis (Laursen & Kristoffersen 1999; Anthonissen 2012). Currently, $\delta^{18}O$ stratigraphy on calcareous benthic foraminifera, which could improve the stratigraphy, is lacking. Despite a few attempts, the magnetostratigraphy of the Miocene succession has not been resolved either and is currently limited to the Oligocene–Miocene boundary interval (Śliwińska *et al.* 2014).

The MCO coincides with a high in global sea level (Miller *et al.* 2020; Rohling *et al.* 2021). In Denmark, the

flooding at the base of the Arnum Fm is considered to be related to the onset of the MCO. However, the precise onset of the MCO in Denmark is still uncertain.

To date, the most complete Miocene succession in Denmark is penetrated by the Sønder (Sdr.) Vium borehole (DGU 102.948; 55°9'04.02" N, 8°24'46.52"E; Fig. 2). The core is located in the western part of the Jylland penisula, Denmark, in the eastern North Sea Basin (Fig. 3). The cored Miocene succession in the Sdr. Vium core consists of shallow and offshore marine to deltaic deposits spanning *c.* 20.4–8 Ma (late Aquitanian – latest Tortonian).

The core has been studied for many years for sedimentology (Rasmussen *et al.* 2010), dinocyst stratigraphy (Dybkjær & Piasecki 2010), foraminifera stratigraphy (Anthonissen 2012), pollen and spores palaeoecology, palaeotemperature and precipitation (Larsson *et al.* 2011) and alkenone-derived SST (Herbert *et al.* 2020). Due to its exceptionally long stratigraphic range, the core has formed the backbone of the Miocene stratigraphic and palaeoenvironmental studies carried out in Denmark. The Sdr. Vium core is the only such core in the northern mid- and high latitudes to penetrate a near continuous Miocene succession. It encompasses in ascending order: the Klintinghoved Fm, Bastrup Fm, Arnum Fm, Odderup Fm, Hodde Fm, Ørnhøj Fm and Gram Fm. The sequence stratigraphic framework for the core is based on the work of Rasmussen (1996) and Rasmussen (1997). The sequence stratigraphic framework was defined for onshore Denmark and was later transferred to the Danish and Norwegian offshore sections (Dybkjær *et al.* 2021). Recent work has shown that the 'D' sequence (Fig. 1) should be infact subdivided into two, referred to here as D1 (Burd100) and D2 (Burd200) sequences. Including this subdivision allows us to correlate the Sdr. Vium core with the sequence stratigraphic framework for the eastern North Sea Basin (Fig. 4), as follows:

1. Sequence Boundary (SB) Burd100 (D1 sequence), depth 182 m based on gamma log data
2. Maximum regressive surface (MRS), depth 132 m based on gamma log
3. Maximum flooding surface (MFS) Burd150 (D1 sequence), depth 131.75 m based on the presence of a 1 mm thick glauconite layer
4. SB Burd200 (D2 sequence), depth 85 m based on gamma log data
5. MFS Burd250 (D2 sequence), depth 76.5 m based on gamma log data
6. SB Lang100 (E sequence), depth 51.9 m based on gamma log
7. MFS Lang150 (E sequence), depth 45 m based on gamma log data
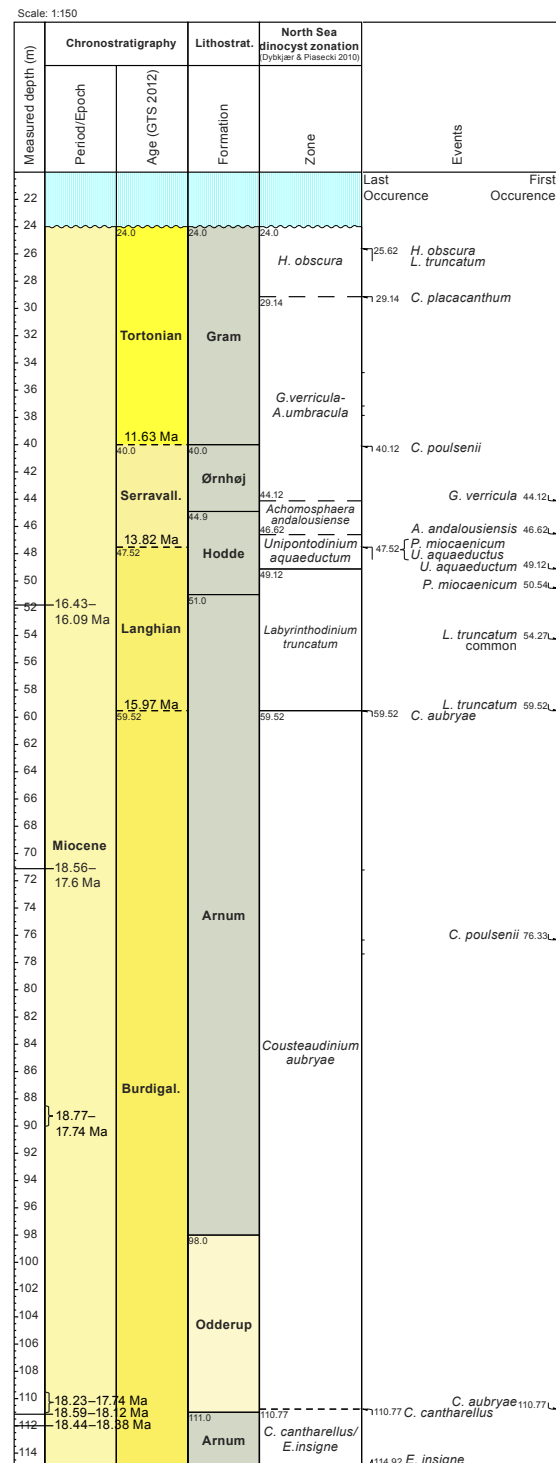
Fig. 2 Stratigraphic framework of the Sdr. Vium borehole (115–24 m depth). Strontium isotope ages from Eidvin *et al.* (2014) are shown in the left column. The ages for the two uppermost samples (51.5–51.8 m and 71.15 m) show ages older than expected from the dinocyst stratigraphic framework, see discussion in Eidvin *et al.* (2014). The Neogene dinocyst zonation by Dybkjær & Piasecki (2010). GTS 2012 from Hilgen *et al.* (2012). First and last occurrences of age-diagnostic dinocysts are shown to the right. **Lithostrat.**: lithostratigraphy. **Serravall.**: Serravallian. **Burdigal.**: Burdigalian. *A. andalousiensis*: *Achomosphaera andalousiensis*. *C. poulsenii*: *Cerebrocysta poulsenii*. *C. placacanthum*: *Cleistosphaeridium placacanthum*. *C. cantharellus*: *Cordosphaeridium cantharellus*. *C. aubryae*: *Cousteaudinium aubryae*. *E. insigne*: *Exochosphaeridium insigne*. *G. verricula*: *Gramocysta verricula*. *H. obscura*: *Hystrichosphaeropsis obscura*. *P. miocaenicum*: *Palaeocystodinium miocaenicum*. *U. aqueductum*: *Unipontidinium aquaeductus*. *L. truncatum*: *Labyrinthodinium truncatum*.
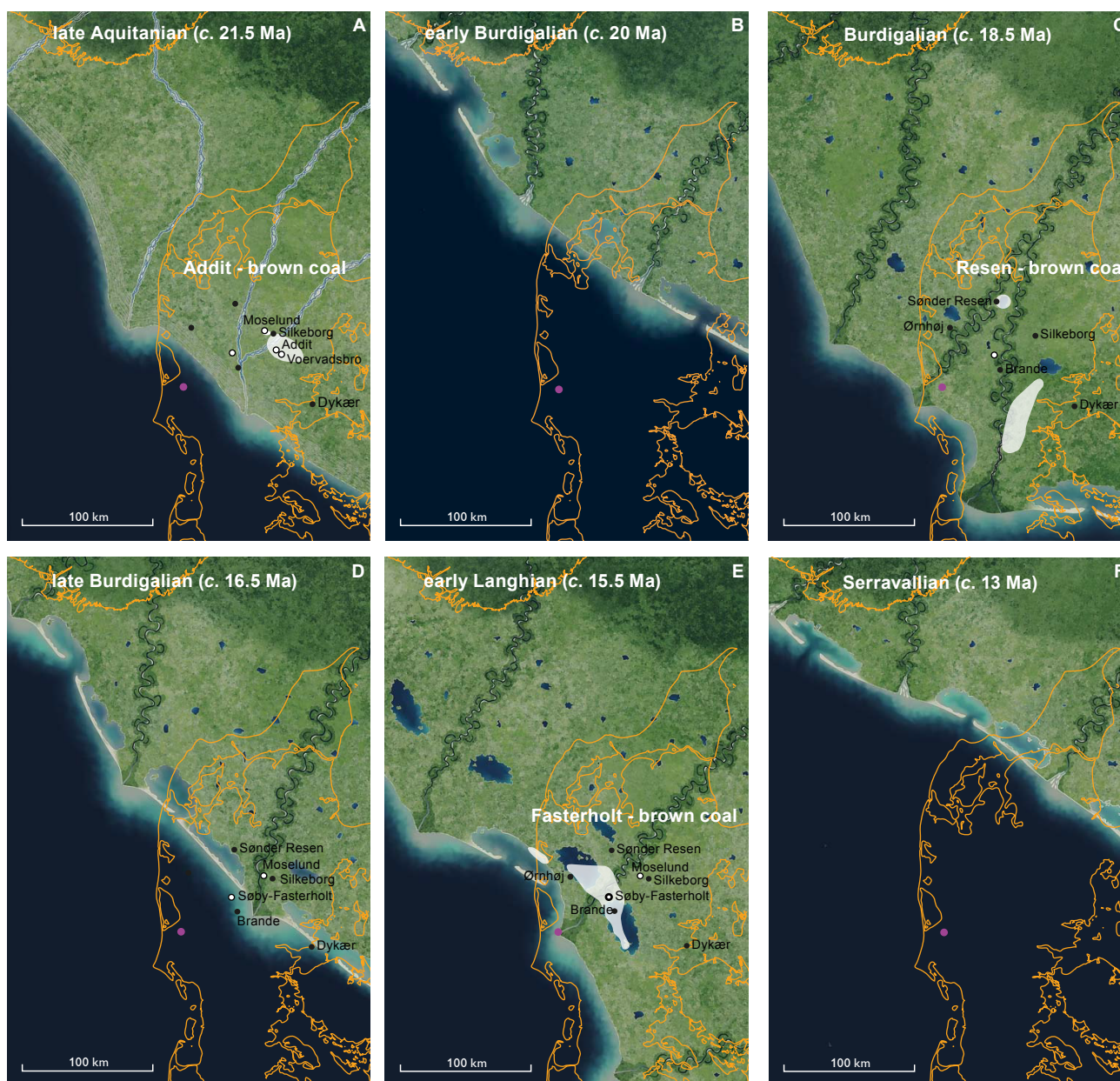
Fig. 3 Palaeogeography of the study area during the late Aquitanian (**A**), early (**B**), mid (**C**) and late Burdigalian (**D**), early Langhian (**E**) and Serravallian (**F**). **White shading** indicates areas where brown coal deposits were reported (after Grambo-Rasmussen (1984) and Rasmussen *et al.* (2010)). **Purple dot**: Sdr. Vium core. Location of place names mentioned in the text is shown as **black dots** (cities) and **white dots** (localities). **Yellow lines** show the coastline today.

8. SB Tort100 (F sequence) at depth 40 m based on gamma log data
9. MFS Tort150 (F sequence), depth *c*. 35 m based on clay mineralogy in the Gram borehole. Clay mineralogic data from Sdr. Vium are missing, and therefore, the position of this MFS is placed approximately.

The biostratigraphic framework for the core was published by Dybkjær & Piasecki (2010; Fig. 2), but the full set of raw data for the core were not published. In this study, we make these data available and have increased the sample resolution for the dinoflagellate dinocyst stratigraphy compared to that originally reported by

Dybkjær & Piasecki (2010). In doing so, all slides were processed following the methods described in Dybkjær (2004). The data set contains raw palynomorph counts and is provided in Supplementary File S1. It includes:

- 42 samples analysed in 2009 by Stefan Piasecki ('SP' in the data set) and included in Dybkjær and Piasecki (2010)
- 10 additional samples analysed in 2022 by Julie Fredsborg ('JMF' in the data set).

First and last occurrences of age-diagnostic dinocysts in the interval from 115 to 24 m are shown in Fig. 2. In
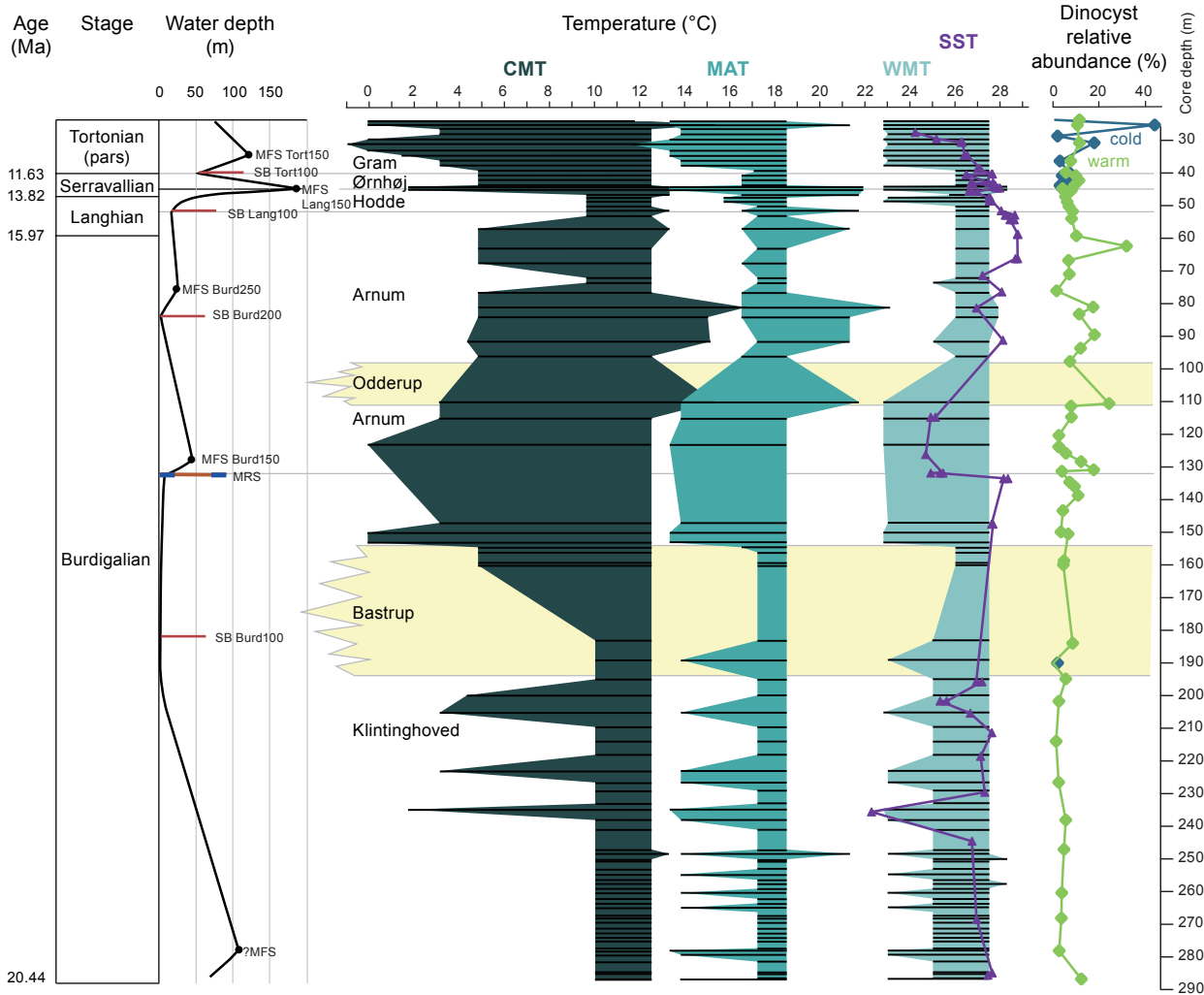
Fig. 4 Temperature evolution recorded in the Sdr. Vium core. **CMT**: coldest month temperature. **MAT**: mean annual temperature. **WMT**: warmest month temperature. **SST**: sea-surface temperature. The temperature ranges are based on the Coexistence Approach (CA) performed on the data set generated by Larsson *et al.* (2010, 2011). SST based on alkenones and plotted after Herbert *et al.* (2020). **Dinocyst relative abundance**: relative distribution of warm- and cold-favouring dinocyst taxa. Dinocyst taxa assigned as warm- and cold-water indicators are shown in Supplementary File S2. **MFS**: maximum flooding surface. **SB**: sequence boundary. **MRS**: maximum regressive surface. **?MFS**: possible MFS.

the interval from 288 to 115 m, we follow the dinocyst events as described in Dybkjær & Piasecki (2010).

3 The geological evolution and palaeogeography of the eastern North Sea Basin

For more than 100 Myr, from the Lower Cretaceous to the Oligocene, the eastern North Sea Basin was covered by an epicontinental sea. During the Oligocene, the North Sea became semi-enclosed, and siliciclastics originating from present-day Scandinavia were deposited. Several of the cooling episodes during the Oligocene are linked to falls in glacioeustatic sea level (Śliwińska *et al.* 2010; Clausen *et al.* 2012). At least one major fluviodeltaic system developed in the northern North Sea Basin during the middle Oligocene (Jarsve *et al.* 2015; Śliwińska 2019). The global cooling at the Oligocene–Miocene boundary related to a fall in glacioeustatic sea level caused a

retraction of the coastline in the area that constitutes present-day Denmark. This resulted in either a hiatus or a condensed section across the boundary interval (e.g. Rasmussen *et al.* 2010; Śliwińska *et al.* 2014).

During the Early Miocene, a major fluviodeltaic system developed in the eastern North Sea Basin (Fig. 3; Ziegler 1990; Rasmussen *et al.* 2010). This change in depositional setting was caused by inversion tectonics (Ziegler 1990; Rasmussen *et al.* 2008; Rasmussen 2009b). Former basins within the area were uplifted, for example, the Central Graben and the Norwegian–Danish Basin. The Norwegian–Danish Basin became shallower and consequently had a physiography perfectly suited to progradation of delta systems from Scandinavia and into the eastern North Sea Basin (Olivarius *et al.* 2015). Deposits of the fluviodeltaic systems consisted of very mature sediments, pure quartz, quartzites, kaolinite and goethite as well as flint. These types of sediments were formed due to exposure and

erosion of old Mesozoic etched basements and chalk in the hinterland (Lidmar-Bergström *et al.* 2000). Based on sediment and mineral provenance studies, the source area is known to have covered the SW part of present-day Norway and central Sweden (Olivarius *et al.* 2015).

3.1 Miocene shoreline

The Miocene landscape of the eastern North Sea was characterised by a NW–SE-trending shoreline (Fig. 3). As a result of global sea-level change and the uplift of Scandinavia (e.g. Rasmussen *et al.* 2008), the coastline migrated NE during highstands and SW during lowstands. Several times, the shoreline moved so far SW that nearly the entire area of present-day Denmark could be classified as emerged lowland. In the earliest part of the Miocene, the fluvial system was characterised by braided rivers but changed to meandering rivers in the later part of the Early Miocene (Rasmussen 2009a; Rasmussen *et al.* 2010). The eastern North Sea Basin was located in the northern westerly wind belt. Consequently, alongshore currents transported sediments dispersed from rivers towards the SE, and spit systems and barrier islands were formed SE of the main delta complexes (Rasmussen & Bruun-Petersen 2010). Muddy sediments were transported NW by deeper marine bottom currents and plastered along the slope (Hübscher *et al.* 2016). Progradation and flooding of these delta systems took place three times during the Early to early Middle Miocene. Vast forested mires developed on these deltas and coastal plains, where abundant plant material accumulated, forming peats and peaty soils during each phase of delta-formation. The mires and the accumulated peat deposits were drowned and buried at the termination of each delta system, allowing the peats to be preserved as the Miocene brown coal deposits we know today (Figs 1, 5). The progradation and flooding of the delta systems were mainly controlled by eustatic sea-level changes (Figs 1, 3; Rasmussen 2004; Miller *et al.* 2005; John *et al.* 2011).

During the early part of the Middle Miocene, a major flood took place in the eastern North Sea Basin. The delta- and coastal plain-dominated environment of the Early Miocene was succeeded by fully marine depositional conditions, such that water depth in the marginal areas of the eastern North Sea Basin reached more than 100 m during the middle part of the Middle Miocene (Rasmussen *et al.* 2010). This flooding of the delta complexes occurred despite a fall in eustatic sea level in the order of 70 m (John *et al.* 2011) and is interpreted to be a consequence of accelerated subsidence of the North Sea Basin during the Middle Miocene (Koch 1989; Rasmussen 2004). The marine conditions continued until the latest Late Miocene. During this period, mud deposition dominated (Nielsen *et al.* 2015), however, with increasing intercalation of laminated silt and fine-grained sand

(Rasmussen & Larsen 1989). During the Late Miocene, the shoreline migrated across present-day Denmark, and fluviodeltaic deposition was re-established (Rasmussen *et al.* 2005, 2010). By the end of the Miocene, delta progradation commenced in the central part of the North Sea Basin (Møller *et al.* 2009).

3.2 Miocene water depth

Water depth can be reconstructed based on the fossil assemblages or established by the mapping of the clinoform break point observed in seismic profiles (Rasmussen *et al.* 2010). The first studies providing estimates of water depth were based on molluscs (Sorgenfrei 1958; Rasmussen 1966, 1968). The most recent studies are based on foraminifera assemblages (Laursen & Kristoffersen 1999) and seismic interpretation (Rasmussen *et al.* 2010).

Overall, water depths during the Miocene were similar to modern-day water depths in the eastern North Sea: predominantly shallow (0–50 m water depth), occasionally up to 150 m deep. The water depth estimations for the Sdr. Vium core are shown in Fig. 4. These are based on regional correlation panels showing the architecture of the Miocene succession, sequence boundaries interpreted to represent subaerial exposure (SBs Burd200 and Lang100), sedimentary facies shift indicating storm wave base (MFS Burd250), seascape morphology from correlation panels and water depth estimation from biofacies studies (foraminifera).

3.3 Miocene brown coals – a terrestrial climate archive

Brown coals (lignite and fossilised peat) consist of partially decayed plant material deposited in stable, wet, shallow areas, with no disturbances by rivers or oceans. Areas where precursor peats formed remained saturated with water, covering dead plant material and protecting the peat from degradation by exposure to atmospheric oxygen. Brown coal consists of the least altered organic material compared to other sediment types. Consequently, brown coals often yield exceptionally well-preserved plant fragments, cuticles, leaves and fruits, as well as pollen and spores (terrestrial palynomorphs). In some cases, entire tree trunks or large tree-log fragments have been found.

Fossilised peats encapsulate information about local floral diversity, temperature and precipitation. Furthermore, brown coal beds provide exceptional sedimentary archives considering that they record long (thousands of years), stable depositional conditions. Thus, they provide unique insights into both large-scale and local-scale changes in depositional conditions, vegetation and climate.

Nearly, all existing brown coal deposits suffer from a poorly constrained stratigraphic framework since

terrestrial palynomorphs are much less accurate for dating sediments, compared with marine microfossils, and brown coal seams are primarily interbedded with sand deposits, which are also very difficult to date precisely.

Brown coal deposits of Miocene age are known from several locations worldwide, including Australia (Holdgate & Clarke 2000), Vietnam (Petersen *et al.* 2022), Greece and Turkey (Kalkreuth *et al.* 1991; Kvaček *et al.* 2002; Güner *et al.* 2017; Bouchal *et al.* 2018; Oskay *et al.* 2019; Denk *et al.* 2022) and India (Singh *et al.* 1992). There are also well-described brown coal deposits in Central and Northern Europe, for example, the lower Rhineland in Germany (Utescher *et al.* 2000, 2002, 2021), Poland (Widera 2016; Dumont *et al.* 2020; Worobiec *et al.* 2021) and Iceland (Grímsson *et al.* 2007; Denk *et al.* 2011). The widespread peat formation in the Miocene might have been associated with high precipitation rates.

For decades, brown coals were studied not only because they provide a detailed, high resolution, local terrestrial climatic record, but mainly in the context of their quality as an energy source. Therefore, the best studied brown coal deposits are in countries with the largest lignite reserves and exploration potential. However, most lignite mines in Europe are now closed or nearly closed as lignite is phased out to reduce global carbon emissions.

Brown coals were studied extensively in Denmark during three exploration campaigns from the 1920s until the 1980s (Koch & Christensen 1979; Grambo-Rasmussen 1984). There are three brown coal-bearing layers of Miocene age recognised in Denmark. Each of the units was deposited as a final stage of the major delta build-up episode (Rasmussen *et al.* 2010). Extensive work carried out on the Miocene deposits in Jylland to map aquifers means that the brown coals of Denmark are relatively well dated, as follows:

1. Brown coal at the top of the Billund Fm (the Addit Mb, late? middle Aquitanian – equivalent to the *Caligodinium amiculum* dinoflagellate cyst Zone; Rasmussen *et al.* 2010, their fig. 7). The age of the zone is estimated to span an interval from ?21.6 to 21.10 Ma (Dybkjær & Piasecki 2010). The maximum cumulative thickness of the brown coals is up to 4 m (Rasmussen pers. comm) but usually 0.5 m (e.g. the Voervadsbro outcrop section; Rasmussen *et al.* 2010). Petrified wood fragments were reported from the brown coal layer of this age (Weibel 1996). Palaeobotanical studies are limited to the lignite clays of Moselund and Silkeborg Vesterskov (Mathiesen 1965, 1970, 1975). Brown coals of this age are known from the area of Addit, SE of Silkeborg (location in Fig. 3A).

2. Brown coal layer at the top of the Bastrup Fm (within the Resen Mb, early Burdigalian – assigned

Fasterholt outcrop
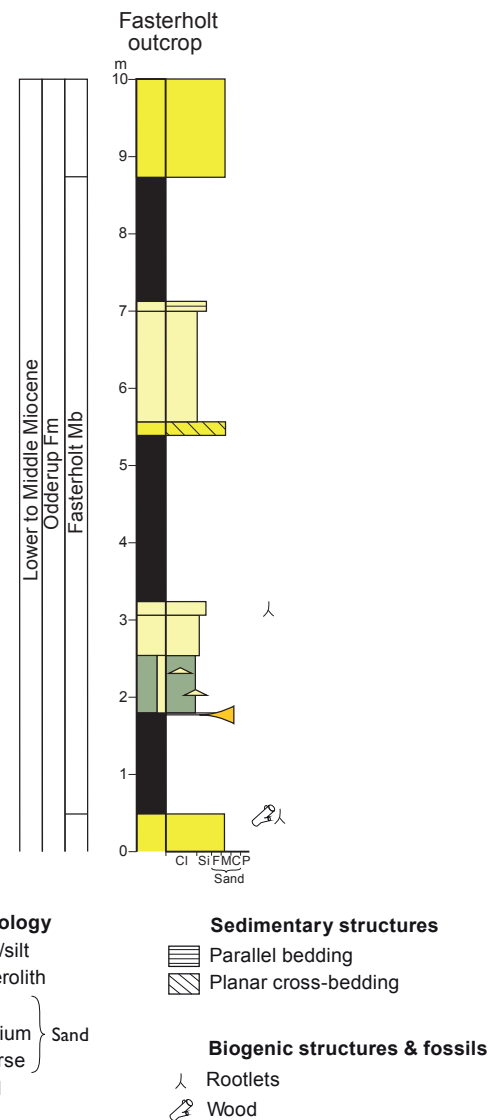
Fig. 5 The type section of the Fasterholt Member is the Fasterholt Brown Coal Pit, northwest of Brande; this section is no longer exposed. The log is redrawn from Koch (1989) and Rasmussen *et al.* (2010). **Cl**: clay. **Si**: silt. **F**: fine sand. **M**: medium sand. **C**: coarse sand. **P**: pebbles.

to the *Cordosphaeridium cantharellus* Zone; Rasmussen *et al.* 2010). The stratigraphic range of the zone is from 19.0 to 18.4 Ma (Dybkjær & Piasecki 2010). The Resen Mb consists of dark brown, organic-rich, silty clay with some coal layers present locally. The coaly layers are often sandwiched between sand-rich units (Rasmussen *et al.* 2010). Brown coal layers 2–3 m thick were mined close to Sønder Resen village between 1914 and 1970 (Sdr. Resen 2023). However, there are no reports of palynofloral studies of coal layers of that age. The brown coals of the Resen Mb are also found in southern Jylland (Fig. 3C).

3. Brown coal at the top of the Odderup Fm (the Fasterholt Mb – assigned to the upper part of the *Labyrinthodinium*

truncatum Zone; Rasmussen *et al.* 2010) is the thickest (Fig. 5) and most spatially spread (Fig. 3E). The zone is dated from 15.97 to 14.8 Ma (Dybkjær & Piasecki 2010). The coals and coal-bearing sediments of the Fasterholt Mb were deposited in freshwater lakes, lagoon swamps and mires (Koch 1989; Rasmussen *et al.* 2010) and are found in several boreholes in central Jylland (Rasmussen *et al.* 2010). The cumulative thickness of the brown coals can be of up to 9 m (Rasmussen pers. comm; Fig. 5). The brown coal-bearing Fasterholt Mb is best exposed at the Abildaa Brown Coal Museum near Ørnhøj. The brown coal of the Fasterholt Mb was extensively mined between 1914 and 1970 to supply national energy resources in Denmark (e.g. Grambo-Rasmussen 1984). The flora described from this coal layer, referred to as the 'Søby-Fasterholt flora' (Koch & Friedrich 1970; Fig. 1) or 'Damgaard flora' (Friis 1979), is so far the best studied of the Miocene brown coal floras in Denmark and represents vegetation during the MCO (see Section 4).

4 Reconstructions of Miocene vegetation

Miocene vegetation reconstructions in Denmark are based on (1) palaeobotanical records comprising dispersed spores and pollen (Aquitanian to Tortonian, Sdr. Vium core; Larsson *et al.* 2006, 2010, 2011) and (2) a rich carpological (fruits and seeds) and leaf record from the Middle Miocene (Langhian) deposits from the Søby-Fasterholt flora in Denmark (Koch & Friedrich 1970, 1971; Koch *et al.* 1973; Wagner & Koch 1974; Friis 1975, 1977, 1985; Christensen 1976; Koch 1989; Denk & Bouchal, 2021a, b).

In this Section, we outline the broad trends in vegetation development and floristic turnover during the Miocene in the present-day Denmark and compare these with the existing palaeobotanical records from Germany and Iceland (Mai 1995; Denk *et al.* 2011). While Miocene floras of Germany are geographically closest to Denmark, the Icelandic Langhian to Messinian macro- and microfloras provide an opportunity to compare North Atlantic European floras along a latitudinal gradient.

During the warm humid conditions that prevailed during the Early and Middle Miocene, coastal vegetation comprised wetlands, swamp forests and diverse, well-drained lowland forests (Larsson *et al.* 2006, 2010, 2011). Vegetation composition during this time differed considerably from the modern Danish flora comprising many woody elements more typical of the present-day distribution in eastern North America and East Asia (Friis 1985; Mai 1995; Larsson *et al.* 2011; Denk & Bouchal 2021a; Supplementary File S2).

The plant fossil record for the MCO is derived from fruits, seeds, leaves and spores and pollen from the Søby-Fasterholt lignite mining area (e.g. Koch & Friedrich 1970; Christensen 1975, 1976; Friis 1985; Koch 1989; Denk & Bouchal, 2021a, b). The record contains a high proportion of plant taxa that would be considered "exotic" today (Supplementary File S3). Exotic elements include genera, which are at present confined to East Asia such as the conifers *Glyptostrobus*, *Sciadopitys* and *Cathaya* (Fig. 6A, B), the broadleaf taxa *Tetracentron* (Figs. 6C, D) and *Platycarya*, a walnut relative. Other genera are currently confined to North America, for example, the lignite forming swamp cypress *Taxodium* and the Redwood, *Sequoia*, the woody angiosperm *Comptonia* (Fig. 6E), and wetland plants *Decodon* (Fig. 6G) and *Dulichium* (Fig. 6H). *Ludwigia* (Fig. 6J), *Cephalanthus* (Fig. 6K) and *Proserpinaca* (Fig. 6L) are also native to Central and South America. Today, the tree genus *Sequoia* (Redwood) is restricted to western North America. In the Denmark, roots assigned to this genus were described from MCO deposits (Wagner & Koch 1974), and leafy shoots and cones were described from pre-MCO deposits (Mathiesen 1970). *Sequoia* thrives today under a Mediterranean-type climate with dry summers and moist winters. It tolerates light frost, and during the summer, it receives a lot of humidity from fog precipitation (Dawson 1998). This additional supply of water during the summer suggests that the original climate niche of *Sequoia* was fully humid temperate.

In Denmark, several taxa in the Early and Middle Miocene plant assemblages represent genera that have a disjunct modern distribution in the Americas and (South) East Asia. Among these are the conifer genus *Tsuga* and the broadleaf taxa Engelhardioideae, *Carya* (walnut relatives), *Magnolia*, *Nyssa*, *Symplocos, Liquidambar* and others. As in the example of *Sequoia*, *Magnolia* is today found in warm temperate to tropical areas of Asia and the Americas but had a wide distribution in Europe during the Miocene. Also, the wetland plant *Saururus* (Fig. 6I) belongs to this group. Subtropical and tropical lineages reported from Aquitanian and Burdigalian pollen assemblages (e.g. the pantropical families Sapotaceae and Arecaceae – the palms; Larsson *et al.* 2006, 2011) are legacies from older periods. This is also true for several extinct taxa in the Søby-Fasterholt flora, for example the monocot genus *Cladiocarya* and various extinct members of the oak family, Fagaceae (Daghlian 1981; Friis 1985; Denk & Bouchal 2021a, b). A single plant genus, *Tetraclinis* in the Cupressaceae family, is today confined to SW Europe and North Africa.

In addition to these exotic plant elements in the Middle Miocene of Denmark, members of the modern flora of Central and Northern Europe make up an important component (*c.* 1/3) of the Søby-Fasterholt flora fossil assemblage. These include the most characteristic tree taxa of the modern flora of Denmark: *Pinus, Fagus, Alnus,*
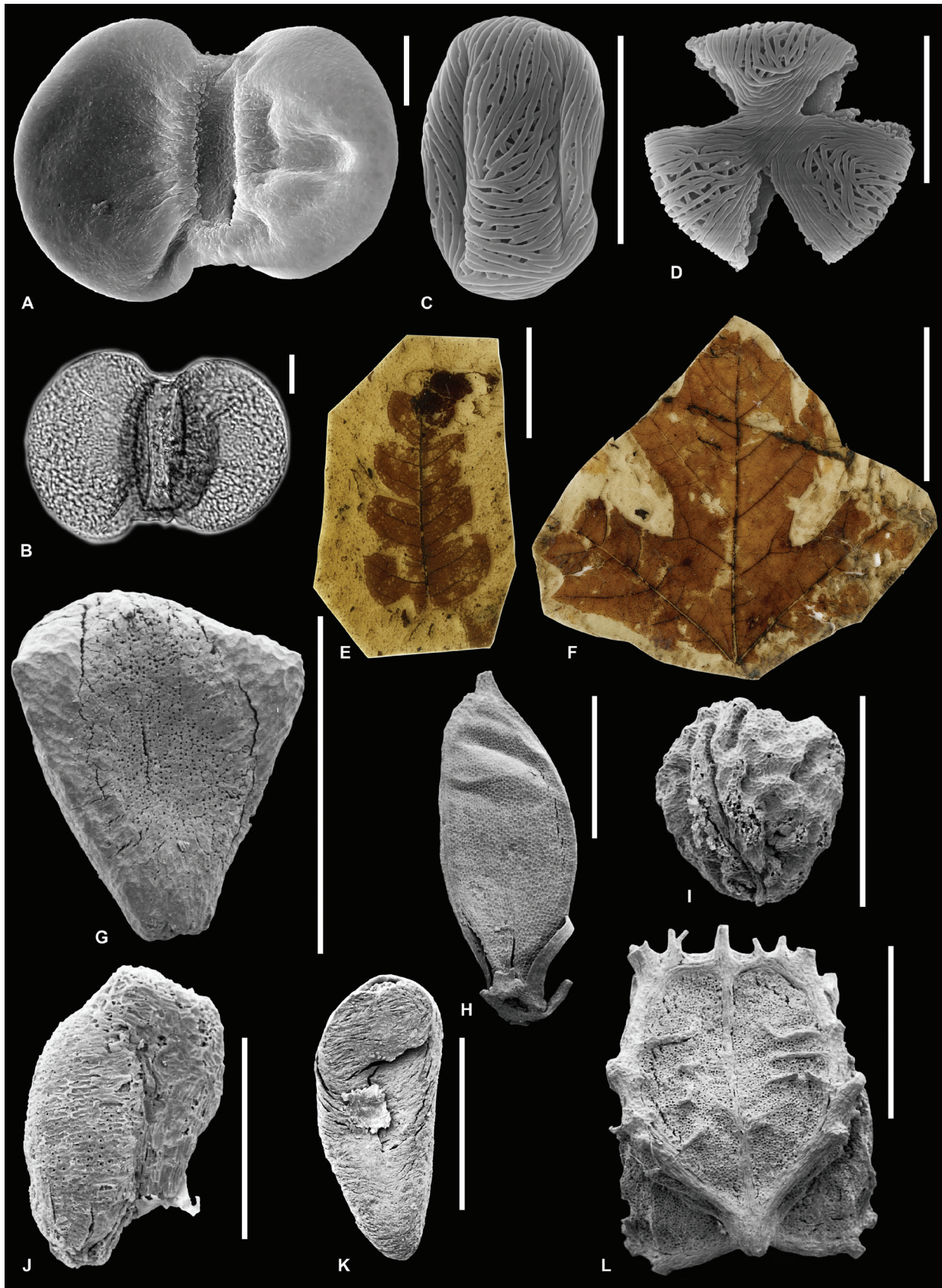
Fig. 6 Typical Middle Miocene plant fossils from the Søby-Fasterholt flora lignite mining area. **A–D**: dispersed pollen grains. **A, B**: *Cathaya* sp. (SEM, LM). **C, D**: *Tetracentron* sp. (SEM, equatorial and polar views). **E–F**: Leaf fossils. **E**: *Comptonia comptoniifolia* (Brongniart) Doweld. **F**: *Acer soebyensis* Christensen nom. inval. **G–L**: Dispersed fruits and seeds. **G**: *Decodon vectensis* Friis, seed. **H**: *Dulichium marginatum* (C. Reid & E.M. Reid) Dorofeev, fruit. **I**: *Saururus bilobatus* (Nikitin ex Dorofeev) Mai, fruitlet. **J**: *Ludwigia corneri* Friis, seed. **K**: *Cephalanthus pusillus Friis*, mericarp. **L**: *Proserpinaca brevicarpa*, Dorofeev endocarp. Scale bars are 10 µm (A–D), 1 cm (E), 5 cm (F), 1 mm (G–I, K, L) and 0.5 mm (J).

Betula, *Acer* and others. These taxa commonly have a disjunct modern distribution in the Northern Hemisphere with large distribution gaps between (eastern) North America, western Eurasia and East Asia. Likewise, plant taxa with a cosmopolitan distribution are also common in the Søby-Fasterholt flora (*c.* 1/3 of the recorded taxa; Supplementary File S4).

Very little is known about the pre-MCO flora in Denmark (e.g. Larsson *et al*. 2011). The lignite clays of Moselund and Silkeborg Vesterskov are associated with the progradation of the Billund Fm and thus are revised here to Aquitanian age. Leaf and wood remains as well as reproductive structures were reported from these lignites (Mathiesen 1965, 1970, 1975). While the Søby-Fasterholt flora represents mainly riparian and wetland vegetation, the assemblage recorded from Moselund and Silkeborg also comprises elements from the well-drained hinterland vegetation (e.g. *Parrotia*, *Daphnogene*; Mathiesen 1965, 1970, 1975).

A marked change in the flora of Denmark occurred at the onset of the Late Miocene (Tortonian stage). Investigations of dispersed spores and pollen show a sharp increase in herbaceous taxa such as the grass family (Poaceae) and in Ericaceae and *Pinus*, and a decrease in Engelhardioideae, extinct Fagaceae (as 'evergreen *Quercus*') and palms (Larsson *et al.* 2011).

The floristic composition of the Miocene flora in Denmark resembles, to some extent, that reported in NE Germany (Mai 1995). In Lower and Middle Miocene strata, many elements are shared with the Danish Miocene (e.g. *Daphnogene*, *Quercus* sect. *Lobatae*, Mastixiaceae (syn. of Nyssaceae) and palms). The palaeobotanical records from radiometrically dated strata of Iceland show that Middle Miocene floras include exotic elements (papillate Cupressaceae, *Cathaya*, *Magnolia*, *Liriodendron* and others; Denk *et al.* 2011) and lack most of the thermophilous plants present in Central Europe and Denmark (e.g. Mastixiaceae). A sharp increase in herbaceous plants is seen in the Tortonian (Late Miocene) in Denmark (Larsson *et al.* 2011), as well as in coeval floras of Iceland, where Tortonian pollen assemblages are dominated by herbaceous taxa and small-leaved Ericaceae (Denk *et al.* 2011). In contrast, mastixioid flora with Lauraceae and other thermophilous elements persist into the Late Miocene further south in Germany (Mai 1995).

In general, the floristic turnover from the Early and Middle Miocene to the Late Miocene appears to reflect a response of the terrestrial vegetation that bordered the northern North Atlantic to global cooling as indicated in the global marine isotopic records (Utescher *et al.* 1997; Westerhold *et al.* 2020). In contrast, the transition from late Early Miocene flora in Denmark to MCO flora, as reflected in spore and pollen assemblages (Larsson *et al.* 2011), is not linked to marked changes in the dominant plant groups. Nevertheless, there is a weak signal of warming starting in the late Burdigalian and continuing into the MCO. For example, sabaloid palms and Mastixiaceae show increased pollen percentages during this period. The same is true for several extinct evergreen Fagaceae (Denk & Bouchal 2021b).

5 Reconstructions of air temperature and precipitation

For most of the Miocene, NW Europe was warm and wet as suggested from records of vertebrates (Mörs 2002; Böhme 2003; Böhme *et al.* 2011; Utescher *et al.* 2011), mammals (Fortelius *et al.* 2014), flora (Mosbrugger *et al.* 2005; Grímsson *et al.* 2007; Bruch *et al.* 2011) and pollen (Pound *et al.* 2011, 2012; Pound & Riding 2016; Pound & McCoy 2021; McCoy *et al.* 2022). High levels of atmospheric moisture are also suggested by fungal assemblages (Pound *et al.* 2022).

Global precipitation patterns in the Miocene are characterised by large amplitudes (e.g. Böhme *et al.* 2011; Utescher *et al.* 2015), and overall the mean annual precipitation (MAP) was 300–1000 mm higher than at present (Böhme *et al.* 2011). In some regions, however, the climate became significantly drier. The onset of aridification in northern China is observed already in the Early Miocene (22 Ma; e.g. Guo *et al.* 2002). Overall, aridification accelerated in the Late Miocene, leading to, for example, the development of the Sahara Desert *c.* 7 Ma (Schuster *et al.* 2006). Aridification of the climate in the Late Miocene associated with the decreasing temperatures at that time was more of a global phenomenon.

Air temperature and precipitation from the Danish Miocene have been studied using the spore and pollen assemblages as well as organic molecular fossils. Collectively, spore and pollen assemblages collected from two localities and one sediment core (Sdr. Vium) cover a time span between *c.* 23.5 and *c.* 8.5 Ma, across the OMT to the upper Tortonian (Larsson *et al.* 2006, 2010, 2011). Notably, the data set originally generated by Larsson *et al.* (2010, 2011) has herein been updated with the latest climate data for the nearest living relatives using the Palaeoflora database and the Coexistence Approach (CA; Utescher *et al.* 2014).

CA analysis of the pollen record from Sdr. Vium indicates that the mean annual air temperature (MAT) was stable during the Miocene (17–18.5°C), with a mean warmest month temperature (WMT) ranging from 23 to 27.5°C, and the mean coldest month temperature (CMT) between 10 and 12.5°C (Fig. 4). However, fluctuations in the Miocene temperature record are inferred from expansions of MAT, CMT and WMT to include colder or warmer temperatures. During the middle to late Burdigalian, the CA analysis indicates that the climate included cooler temperatures, as plants requiring

milder winter temperatures, such as Mastixiaceae and *Sabal* (palms), were absent from the pollen record. A similar pattern is observed in the Serravallian and Tortonian (Fig. 4). During the latest Burdigalian and Langhian, the presence of Mastixiaceae pollen, in particular, indicates slightly warmer winter temperatures (Fig. 4). Fluctuations in WMT correspond rather well with fluctuations in the SST (see Section 6).

An alternative tool for estimating MAT is based on the distribution of membrane lipids derived from soil bacteria (the branched Glycerol Dialkyl Glycerol Tetraethers; brGDGT). In Denmark, MAT derived from brGDGT has so far been calculated only across the OMT (Śliwińska *et al.* 2014). Between 24.5 and *c.* 22.5 Ma, MAT ranged from 18 to 20°C (excluding the temperature minimum of 16.5–17°C related to the cooling event at the OMT). The brGDGT-derived temperature is similar (i.e. 17–20°C) to air temperature estimations based on the pollen and spores from the Dykær locality, Denmark (palynomorphs; Larsson *et al.* 2010; this paper) as well as from other sites in NW Europe, for example fossil leaf floras (Uhl *et al.* 2007; Uhl & Herrmann 2010) and megafloras (Mosbrugger *et al.* 2005). However, recent progress in understanding the origin of brGDGTs and improvements in calibrations for calculating palaeo-temperature call for a new analysis of the existing data set.

Overall, air temperature in the Miocene was significantly higher than today. For comparison, MAT (between 1981 and 2010) in Denmark is 8.3°C (CMT = 1.0°C and occured in February; WMT = 16.6°C and occured in July; Cappelen 2021).

Warm air temperature in Central Europe during the Miocene is indicated by numerous published vegetation records. Palynological results from Germany indicate a warm temperate to subtropical climate during the Miocene (Zetter 1997; Kolcon & Sachsenhofer 1999; Kovar-Eder *et al.* 2001). Palynological and palaeobotanical records from MCO brown coal seams in the Lower Rhine Basin indicate MAP of 1300–2000 mm and MAT *c.* 16–20°C (Utescher *et al.* 2021). In the Lower Rhine Basin, WMT during the MCO exceeded 25°C and sometimes reached 28°C (Utescher *et al.* 2021). This is similar to the pollen-derived climate data from Sdr. Vium (Fig. 4).

CA analysis of the pollen record from Sdr. Vium indicates MAP *c.* 750–1750 mm for much of the Miocene, which is much higher than the *c.* 749 mm observed over the past two decades in Denmark. For the period 1981–2020, April is the driest month in Denmark (mean monthly precipitation, MMP = 37.3 mm). The wettest month is October (MMP = 84.5 mm; Cappelen 2021). Overall, MMP for the driest month during the Miocene ranges from *c.* 5 to 60 mm, while the wettest month ranges from 150 to 250 mm (Fig. 7). Notably, several spikes in MMP for the wettest month are observed from the late Burdigalian (from *c.* 115 m depth in the Sdr. Vium core; Fig. 7). Both MAP and wettest month MMP were thus significantly higher during the MCO than today, while rainfall during the driest month is within the range observed in the Miocene. Notably, the anomalously high rainfall of *c.* 150 mm reported in Denmark in October 2023 reached the lower end of the reconstructed wettest month MMP for the Miocene (150–250 mm).

The high precipitation and warm temperatures (see also SST in Section 6) in the Miocene must have commonly caused storms in the eastern North Sea Basin. In several localities around Denmark, the Miocene succession yields hummocky cross-stratified strata, which suggest that intense storms were common (Rasmussen *et al.* 2010). However, it is not possible to determine if the intensity of storms changed throughout the Miocene.

6 Reconstructions of SST

The SST estimations from the Sdr. Vium core suggest temperatures of up to 28°C, 20.4–12 Ma (Early to Middle Miocene), followed by a gradual decrease to *c.* 24°C, 12–8 Ma (Late Miocene; Fig. 4; Herbert *et al.* 2020). Here (Fig. 8), we follow the age model (absolute ages) proposed by Herbert *et al.* (2020). SST is derived from alkenone palaeothermometry (U^K_{37} index defined by Prahl & Wakeham 1987). Overall, temperature trends for the Sdr. Vium core agree with SST records from six other sites in the North Atlantic region (Fig. 8). However, on closer inspection, pre-MCO temperatures were already high (25–28°C), with no apparent trend in time. Notably, just before the onset of the MCO, a brief interval of lower temperatures (i.e. the SST minimum; 24–25.5°C) marks the most pronounced feature of the SST trend for Denmark. This SST minimum is observed at sites 608, 982 and the Sdr. Vium core – the only sites covering the MCO onset. No major increase in SST related to the onset of the MCO was observed at any of these three sites (Fig. 8). Discrepancies in the timing of the SST minimum may be related either to uncertainties in the age models (especially for the Sdr. Vium core; see Herbert *et al.* 2020 for details) or because these sites are in a region of dynamic oceanic circulation intensity and at the northern extent of the subtropical gyre. Overall, an improved high resolution stratigraphic framework (magneto- or isotope stratigraphy) would significantly aid in explaining these trends.

We could speculate that the SST minimum is related to a colder interval just prior to the MCO, as observed in the sedimentary records from offshore Antarctica (Levy *et al.* 2016). However, we observe that the SST minimum is observed only in the sites bathed by the modern-day subtropical gyre, while site U1406, which is under a subpolar gyre regime, shows a gradual temperature increase in the time-equivalent interval. We
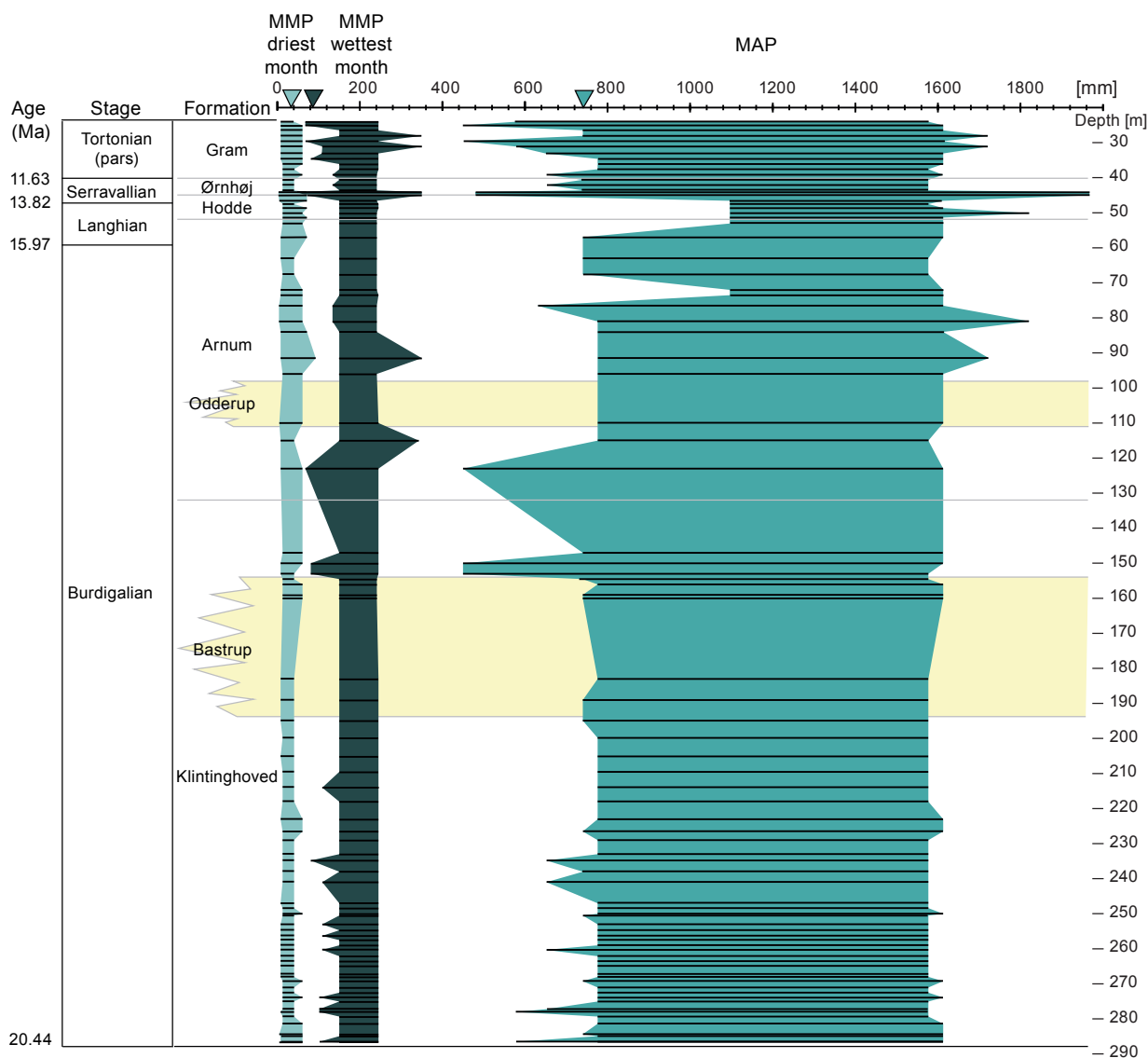
Fig. 7 Precipitation trends derived from Coexistence Approach (CA) on the updated pollen and spore record from the Sdr. Vium core, generated by Larsson *et al.* (2010, 2011). **Dark green triangle**: mean annual precipitation (**MAP**) in Denmark, 1981–2020 (*c.* 749 mm; Cappelen 2021). **Lightest green triangle**: mean monthly precipitation (**MMP**) for the driest month (April; 37.3 mm). **Light green triangle:** MMP for the wettest month (October; 84.5 mm).

could, therefore, argue that the SST minimum observed in the eastern North Atlantic associated with warming in the western North Atlantic (reorganisation of the subtropical gyre) was an effect of weakening of the oceanic circulation in the North Atlantic rather than an overall cooling. However, this would need to be supported by, for example, modelling.

7 The onset of MCO and the Middle to Late Miocene transition

Following the age model applied by Herbert *et al.* (2020), the onset of the MCO is placed at the onset of warmer SST (approximately at depth 90 m in the Sdr. Vium core). However, both dinocyst assemblages (showing a flux of warm water taxa) and pollen and spore assemblages suggest that warming occurred earlier and stepwise. The relative abundance of warm water dinocysts shows an

initial increase at *c.* 130 m depth and another increase at 110 m (Fig. 3). The first flux of warm water dinocysts at 130 m corresponds with the MFS at the base of the Arnum Fm, which is considered to be synchronous with the global sea-level rise at the onset of MCO. However, SST derived from alkenones record a sharp decrease at that depth, which contradicts the dinocyst records. Our climate inferences based on the palynological record suggest at least three warming steps: (1) at depth 110 m, associated with a slight increase in the relative abundance of palm pollen, (2) at 90 m, where the abundance of warmth-loving deciduous Fagaceae ('*Castanea*' in Larsson *et al.* 2011) increased, and (3) at 75 m, where sabaloid palms, Engelhardioideae and the evergreen *Fagaceae* showed a marked increase.

The transition from the Middle to the Late Miocene is well expressed in our inferred palaeoclimate data
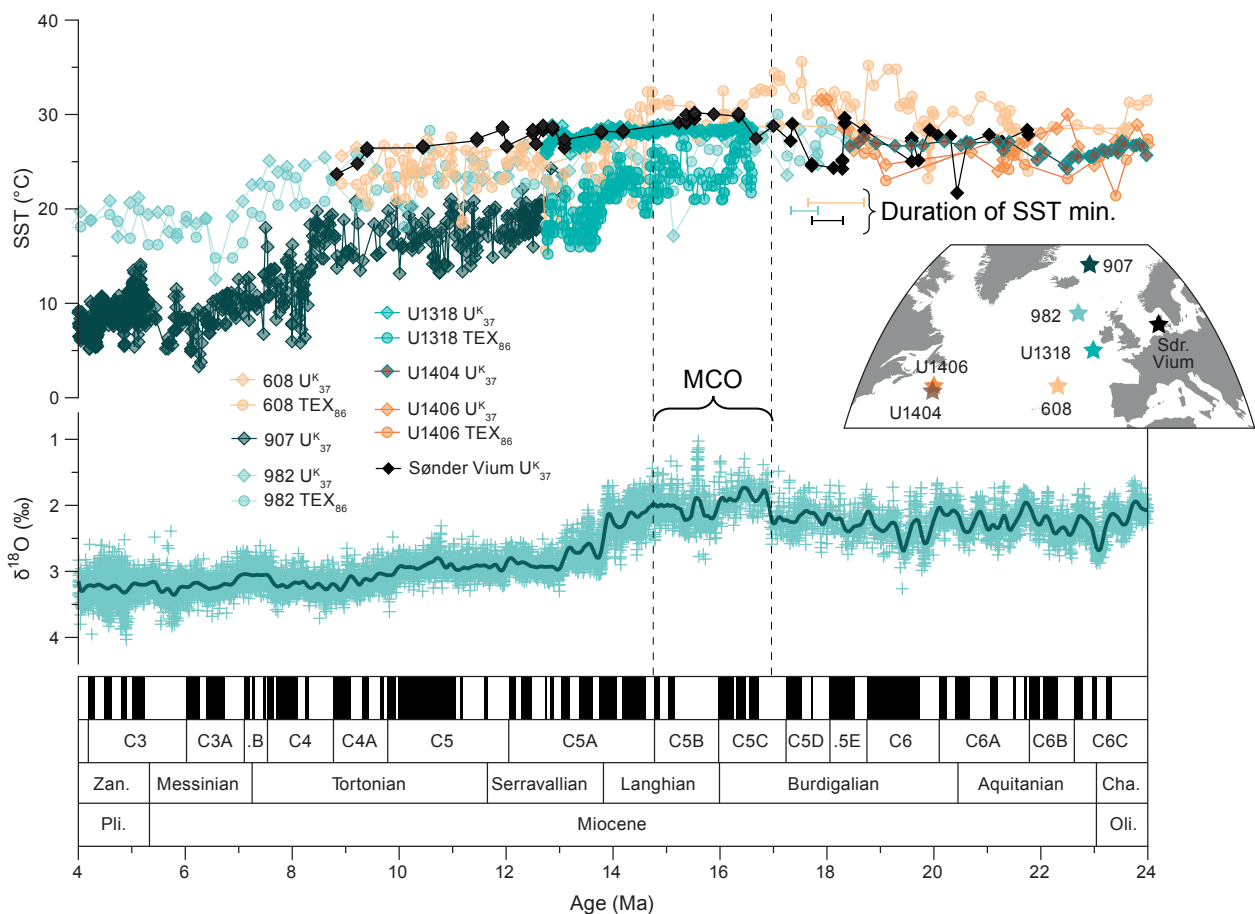
Fig. 8 Compilation of existing sea-surface temperature (**SST**) records from the northern low to high latitudes. Sites are as follows: Deep Sea Drilling Program (DSDP) Site 608, Ocean Drilling Program (ODP) Site 907, ODP Site 982, Integrated Ocean Drilling Program (IODP) Site U1318, IODP Site U1404, IODP Site U1406 and Sdr. Vium core. Data sources: Herbert *et al.* (2016, 2020); Liu *et al.* (2018); Super *et al.* (2018, 2020); Guitián *et al.* (2019); Sangiorgi *et al.* (2021). Also shown is the global composite oxygen isotope curve (**δ¹⁸O**) for benthic foraminifera (Westerhold *et al.* 2020) across the Miocene. **MCO**: Miocene Climatic Optimum. **Cha.**: Chattian. **Oli.**: Oligocene. **Plio.**: Pliocene. **Zan.**: Zanclean. **C3–C6**: polarity chrones. **UK₃₇**: Unsaturated long-chain Ketones index with 37 carbon atoms (C37 alkenones). **TEX₈₆**: tetraether index of 86 carbon atoms.

and in corresponding species turnover in the terrestrial and marine realms. In the plant fossil record, this transition is reflected in a marked decrease of taxodiaceous Cupressaceae, and an increase in cold-tolerant woody taxa, such as *Carya*, Ericaceae and Poaceae. Likewise, the post-MCO cooling trend in surface water temperature is recorded by the alkenones and the sharp increase in cold-tolerant dinocysts.

8 Conclusions

The MCO is the most recent time in Earth history where the CO_2 levels were as high as today. All the existing data from the Danish Miocene succession suggest that the area was significantly warmer and wetter than today. However, recent anomalies in rainfall (such as the massive rainfall in October 2023) reach the minimum values recorded for MMP during the wettest month in the Miocene.

The onset of the MCO in the eastern North Sea Basin seems to be related to a sequence of warming steps or pulses in both the marine and terrestrial realms. Some of these steps are synchronous, some are not.

However, the main obstacle in the evaluation of these is the fact that the existing data sets are either of too low resolution or have different sampling depths. Another improvement in resolving the Miocene climate record for the eastern North Sea Basin could be to provide an integrated magnetostratigraphic age model for the Danish Miocene.

Additional information

Additional files

Four supplementary files are available at *https://doi.org/10.22008/FK2/T1YJC4*. **Supplementary File S1**: raw polymorph counts. **Supplementary File S2**: Full data set of dinocyst raw counts plotted using StrataBugs program. **Supplementary File S3**: Raw pollen counts. **Supplementary File S4**: Søby Fasterholt and Moselund Silkeborg floras. **Supplementary S5**: Sdr. Vium CA-derived estimations for precipitation and temperature.

References

Anagnostou, E., John, E.H., Edgar, K.M., Foster, G.L., Ridgwell, A., Inglis, G.N., Pancost, R.D., Lunt, D.J. & Pearson, P.N. 2016: Changing atmospheric CO_2 concentration was the primary driver of early Cenozoic climate. Nature **533**, 380–384. *https://doi.org/10.1038/nature17423*

Anthonissen, E.D. 2012: A new Miocene biostratigraphy for the northeastern North Atlantic: an integrated foraminiferal, bolboformid, dinoflagellate and diatom zonation. Newsletters on Stratigraphy **45**, 281–307. *https://doi.org/10.1127/0078-0421/2012/0025*

Badgley, C., Barry, J.C., Morgan, M.E., Nelson, S.V., Behrensmeyer, A.K., Cerling, T.E. & Pilbeam, D. 2008: Ecological changes in Miocene mammalian record show impact of prolonged climatic forcing. Proceedings of the National Academy of Sciences **105**, 12145–12149. *https://doi.org/10.1073/pnas.0805592105*

Böhme, M. 2003: The Miocene Climatic Optimum: evidence from ectothermic vertebrates of Central Europe. Palaeogeography, Palaeoclimatology, Palaeoecology **195**, 389–401. *https://doi.org/10.1016/S0031-0182(03)00367-5*

Böhme, M., Winklhofer, M. & Ilg, A. 2011: Miocene precipitation in Europe: temporal trends and spatial gradients. Palaeogeography, Palaeoclimatology, Palaeoecology **304**, 212–218. *https://doi.org/10.1016/j.palaeo.2010.09.028*

Bouchal, J.M., Güner, T.H. & Denk, T. 2018: Middle Miocene climate of southwestern Anatolia from multiple botanical proxies. Climate of the Past **14**, 1427–1440. *https://doi.org/10.5194/cp-14-1427-2018*

Bruch, A.A., Utescher, T. & Mosbrugger, V. 2011: Precipitation patterns in the Miocene of Central Europe and the development of continentality. Palaeogeography, Palaeoclimatology, Palaeoecology **304**, 202–211. *https://doi.org/10.1016/j.palaeo.2010.10.002*

Cappelen, J. (ed.) 2021: Denmark – DMI historical climate data collection 1768–2020. DMI Report 21-02 Danish Meteorological Institute. *https://www.dmi.dk/fileadmin/Rapporter/2021/DMIRep21-02.pdf*

Cerling, T.E., Wang, Y. & Quade, J. 1993: Expansion of C4 ecosystems as an indicator of global ecological change in the late Miocene. Nature **361**, 344–345. *https://doi.org/10.1038/361344a0*

Christensen, E.F. 1975: The Søby Flora: Fossil plants from the Middle Miocene delta deposits of the Søby–Fasterholt area, Central Jutland, Denmark. Part I. Danmarks Geologiske Undersøgelse II. Række **103**, 1–41. *https://doi.org/10.34194/raekke2.v103.6894*

Christensen, E.F. 1976: The Søby Flora: Fossil plants from the Middle Miocene delta deposits of the Søby–Fasterholt area, Central Jutland, Denmark. Part II. Danmarks Geologiske Undersøgelse II Raekke **108**, 4–75. *https://doi.org/10.34194/raekke2.v108.6899*

Clausen, O.R., Śliwińska, K.K. & Gołędowski, B. 2012: Oligocene climate changes controlling forced regression in the eastern North Sea. Marine and Petroleum Geology **29**, 1–14. *https://doi.org/10.1016/j.marpetgeo.2011.10.002*

Collins *et al*. 2013: Long-term Climate Change: Projections, Commitments and Irreversibility. In: Stocker *et al*. (eds): Climate Change 2013: The Physical Science Basis. Contribution of Working Group I to the Fifth Assessment Report of the Intergovernmental Panel on Climate Change.

Cristini, L., Grosfeld, K., Butzin, M. & Lohmann, G. 2012: Influence of the opening of the Drake Passage on the Cenozoic Antarctic Ice Sheet: a modeling approach. Palaeogeography, Palaeoclimatology, Palaeoecology **339–341**, 66–73. *https://doi.org/10.1016/j.palaeo.2012.04.023*

Daghlian, C.P. 1981: A review of the fossil record of monocotyledons. Botanical Review **47**, 517–555. *https://doi.org/10.1007/BF02860540*

Dawson, T.E. 1998: Fog in the California Redwood Forest: ecosystem inputs and use by plants. Oecologia **117**, 476–485. *https://doi.org/10.1007/s004420050683*

Denk, T. & Bouchal, J.M. 2021a: Dispersed pollen and calyx remains of *Diospyros* (Ebenaceae) from the middle Miocene 'Plant beds' of Søby, Denmark. GFF **143**, 292–304. *https://doi.org/10.1080/11035897.2021.1907443*

Denk, T. & Bouchal, J.M. 2021b: New Fagaceous pollen taxa from the Miocene Søby flora of Denmark and their biogeographic implications. American Journal of Botany **108**, 1500–1524. *https://doi.org/10.1002/ajb2.1716*

Denk, T., Grímsson, F., Zetter, R. & Símonarson, L.A. 2011: Late Cainozoic Floras of Iceland. 15 Million Years of Vegetation and Climate History in the Northern North Atlantic. In: Landman, N.H., Harries, PJ (eds): Topics in Geobiology 35, 1–870. *https://doi.org/10.1007/978-94-007-0372-8*

Denk, T., Güner, H.T. & Bouchal, J.M. 2022: Catalogue of revised and new plant macrofossils from the Aquitanian–Burdigalian of Soma (W Turkey) – biogeographic and palaeoclimatic implications. Review of Palaeobotany and Palynology **296**, 104550. *https://doi.org/10.1016/j.revpalbo.2021.104550*

Dumont, H.J., Pociecha, A., Zawisza, E., Szeroczyńska, K., Worobiec, E. & Worobiec, G. 2020: Miocene cladocera from Poland. Scientific Reports **10**, 12107. *https://doi.org/10.1038/s41598-020-69024-9*

Dybkjær, K. 2004: Dinocyst stratigraphy and palynofacies studies used for refining a sequence stratigraphic model – uppermost Oligocene to lower Miocene, Jylland, Denmark. Review of Palaeobotany and Palynology **131**, 201–249. *https://doi.org/10.1016/j.revpalbo.2004.03.006*

Dybkjær, K. & Piasecki, S. 2010: Neogene dinocyst zonation for the eastern North Sea Basin, Denmark. Review of Palaeobotany and Palynology **161**, 1–29. *https://doi.org/10.1016/j.revpalbo.2010.02.005*

Dybkjær, K., Rasmussen, E.S., Eidvin, T., Grøsfjeld, K., Riis, F., Piasecki, S. & Śliwińska, K.K. 2021: A new stratigraphic framework for the Miocene – Lower Pliocene deposits offshore Scandinavia: A multiscale approach, Geological Journal **56** 1699–1725. *https://doi.org/10.1002/gj.3982*

Eidvin, T., Riis, F. & Rasmussen, E.S. 2014: Oligocene to Lower Pliocene deposits of the Norwegian continental shelf, Norwegian Sea, Svalbard, Denmark and their relation to the uplift of Fennoscandia: A synthesis, Marine and Petroleum Geology **56**, 184–221. *https://doi.org/10.1016/j.marpetgeo.2014.04.006*

Flower, B.P. & Kennett, J.P. 1994: The middle Miocene climatic transition: East Antarctic ice sheet development, deep ocean circulation and global carbon cycling. Palaeogeography, Palaeoclimatology, Palaeoecology **108**, 537–555. *https://doi.org/10.1016/0031-0182(94)90251-8*

Fortelius, M., Eronen, J.T., Kaya, F., Tang, H., Raia, P. & Puolamäki, K. 2014: Evolution of Neogene Mammals in Eurasia: environmental forcing and biotic interactions. Annual Review of Earth and Planetary Sciences **42**, 579–604. *https://doi.org/10.1146/annurev-earth-050212-124030*

Friis, E.M. 1975: Climatic implications of microcarpological analyses of the Miocene Fasterholt flora, Denmark. Bulletin of the Geological Society of Denmark **24**, 179–192.

Friis, E.M. 1977: Leaf whorls of Cupressaceae from the Miocene Fasterholt flora, Denmark. Bulletin of the Geological Society of Denmark **26**, 11. *https://doi.org/10.37570/bgsd-1976-26-08*

Friis, E.M. 1979: The Damgaard flora: a new middle Miocene flora from Denmark. Bulletin of the Geological Society of Denmark **27**, 117–142. *https://doi.org/10.37570/bgsd-1978-27-12*

Friis, E.M. 1985: Angiosperm Fruits and Seeds from the Middle Miocene of Jutland (Denmark). Biologiske Skrifter **24**, 1–165.

Goldner, A., Herold, N. & Huber, M. 2014: The challenge of simulating the warmth of the mid-Miocene climatic optimum in CESM1. Climate of the Past **10**, 523–536. *https://doi.org/10.5194/cp-10-523-2014*

Grambo-Rasmussen, A. 1984: Danmarks brunkulsreserver. Rapport Fase 2. Udført for Energiministeriet. Danmarks Geologiske Undersøgelse Serie D **2**, 1–67. *https://doi.org/10.34194/seried.v2.7119*

Grímsson, F., Denk, T. & Símonarson, L.A. 2007: Middle Miocene floras of Iceland — the early colonization of an island? Review of

Palaeobotany and Palynology **144**, 181–219. *https://doi.org/10.1016/j.revpalbo.2006.07.003*

Guitián, J., Phelps, S., Polissar, P.J., Ausín, B., Eglinton, T.I. & Stoll, H.M. 2019: Midlatitude temperature variations in the Oligocene to early Miocene. Paleoceanography and Paleoclimatology **34**, 1328–1343. *https://doi.org/10.1029/2019PA003638*

Güner, T.H., Bouchal, J.M., Köse, N., Göktas, F., Mayda, S. & Denk, T. 2017: Landscape heterogeneity in the Yatağan Basin (southwestern Turkey) during the middle Miocene inferred from plant macrofossils. Palaeontographica Abteilung B **296**, 113–171. *https://doi.org/10.1127/palb/296/2017/113*

Guo, Z.T. *et al.* 2002: Onset of Asian desertification by 22 Myr ago inferred from loess deposits in China. Nature **416**, 159–163. *https://doi.org/10.1038/416159a*

Herbert, T.D., Lawrence, K.T., Tzanova, A., Peterson, L.C., Caballero-Gill, R. & Kelly, C.S. 2016: Late Miocene global cooling and the rise of modern ecosystems. Nature Geoscience **9**, 843–847. *https://doi.org/10.1038/ngeo2813*

Herbert, T.D., Rose, R., Dybkjær, K., Rasmussen, E.S. & Śliwińska, K.K. 2020: Bi-Hemispheric warming in the Miocene climatic optimum as seen from the Danish North Sea. Paleoceanography and Paleoclimatology **35**, e2020PA003935. *https://doi.org/10.1029/2020PA003935*

Hilgen, F.J., Lourens, L.J. & Van Dam, J.A. 2012: The Neogene Period. In: Gradstein, F.M., Ogg, J.G., Schmitz, M.D. & Ogg G.M. (eds): The Geologic Time Scale 2012, Elsevier, 409–440. *https://doi.org//10.1016/B978-0-444-59425-9.00029-9*

Holbourn, A., Kuhnt, W., Schulz, M., Flores, J.-A. & Andersen, N. 2007: Orbitally-paced climate evolution during the middle Miocene "Monterey" carbon-isotope excursion, Earth and Planetary Science Letters **261**, 534–550. *https://doi.org/10.1016/j.epsl.2007.07.026*

Holdgate, G.R. & Clarke, J.D.A. 2000: A review of tertiary brown coal deposits in Australia: their depositional factors and Eustatic correlations. AAPG Bulletin **84**, 1129–1151. *https://doi.org/10.1306/A9673C5C-1738-11D7-8645000102C1865D*

Hübscher, C., Betzler, C. & Reiche, S. 2016: Seismo-stratigraphic evidences for deep base level control on middle to late Pleistocene drift evolution and mass wasting along southern Levant continental slope (Eastern Mediterranean). Marine and Petroleum Geology **77**, 526–534. *https://doi.org/10.1016/j.marpetgeo.2016.07.008*

Hutchinson, D.K., Coxall, H.K., O'Regan, M., Nilsson, J., Caballero, R. & de Boer, A.M. 2019: Arctic closure as a trigger for Atlantic overturning at the Eocene–Oligocene Transition. Nature Communications **10**, 3797. *https://doi.org/10.1038/s41467-019-11828-z*

Jarsve, E.M., Eidvin, T., Nystuen, J.P., Faleide, J.I., Gabrielsen, R.H. & Thyberg, B.I. 2015: The Oligocene succession in the eastern North Sea: basin development and depositional systems. Geological Magazine **152**, 668–693. *https://doi.org/10.1017/S0016756814000570*

John, C.M., Karner, G.D., Browning, E., Leckie, R.M., Mateo, Z., Carson, B. & Lowery, C. 2011: Timing and magnitude of Miocene eustasy derived from the mixed siliciclastic-carbonate stratigraphic record of the northeastern Australian margin. Earth and Planetary Science Letters **304**, 455–467. *https://doi.org/10.1016/j.epsl.2011.02.013*

Kalkreuth, W., Kotis, T., Papanicolaou, C. & Kokkinakis, P. 1991: The geology and coal petrology of a Miocene lignite profile at Meliadi Mine, Katerini, Greece. International Journal of Coal Geology **17**, 51–67. *https://doi.org/10.1016/0166-5162(91)90004-3*

Kasbohm, J. & Schoene, B. 2018: Rapid eruption of the Columbia River flood basalt and correlation with the mid-Miocene climate optimum. Science Advances **4**, eaat8223. *https://doi.org/10.1126/sciadv.aat8223*

King, C., Gale, A.S. & Barry, T.L. 2016: A revised correlation of Tertiary rocks in the British Isles and adjacent areas of NW Europe. Geological Society Special Report **27**, 583 pp. *https://doi.org/10.1144/SR27*

Knorr, G., Butzin, M., Micheels, A. & Lohmann, G. 2011: A warm Miocene climate at low atmospheric CO_2 levels. Geophysical Research Letters **38**, L20701. *https://doi.org/10.1029/2011GL048873*

Koch, B.E. 1989: Geology of the Søby-Fasterholt area: a paleontological and geological investigation on the Miocene browncoal bearing sequence of the Søby-Fasterholt area, Central Jutland, Denmark.

Danmarks Geologiske Undersøgelse Serie A **22**, 170 pp. *https://doi.org/10.34194/seriea.v22.7042*

Koch, B.E. & Christensen, E.F. 1979: Introduction to the symposium 'The continental Miocene of Central Jutland (Denmark)': geology, brown coal facies, stratigraphy, paleontology. Aarhus University, 11–16 June 1979, Aarhus. 97 pp.

Koch, B.E. & Friedrich, W.L. 1970: Geologisch-paläontologische Untersuchung der miozänen Braunkohlen bei Fasterholt in Jutland, Dänemark. Bulletin of the Geological Society of Denmark **20**, 169–191.

Koch, B.E. & Friedrich, W.L. 1971: Früchte und Samen von *Spirematospermum* aus der miozänen Fasterholt-Flora in Dänemark. Palaeontographica Abteilung B **136**, 1–46.

Koch, B.E., Friedrich, W.L., Christensen, E.F. & Friis, E.M. 1973: Den miocæne brunkulsflora og dens geologiske miljø i Søby–Fasterholt området sydøst for Herning. 57 pp. Reitzel.

Kolcon, I. & Sachsenhofer, R.F. 1999: Petrography, palynology and depositional environments of the early Miocene Oberdorf lignite seam (Styrian Basin, Austria). International Journal of Coal Geology **41**, 275–308. *https://doi.org/10.1016/S0166-5162(99)00023-3*

Kovar-Eder, J., Kvaček, Z. & Meller, B. 2001: Comparing Early to Middle Miocene floras and probable vegetation types of Oberdorf N Voitsberg (Austria), Bohemia (Czech Republic), and Wackersdorf (Germany). Review of Palaeobotany and Palynology **114**, 83–125. *https://doi.org/10.1016/S0034-6667(00)00070-1*

Kvaček, Z., Velitzelos, D. & Velitzelos, E. 2002: Late Miocene Flora of Vegora Macedonia N. Greece. University of Athens, Greece. 175 pp.

Larsson, L.M., Dybkjær, K., Rasmussen, E.S., Piasecki, S., Utescher, T. & Vajda, V. 2011: Miocene climate evolution of northern Europe: A palynological investigation from Denmark. Palaeogeography, Palaeoclimatology, Palaeoecology **309**, 161–175. *https://doi.org/10.1016/j.palaeo.2011.05.003*

Larsson, L.M., Vajda, V. & Dybkjær, K. 2010: Vegetation and climate in the latest Oligocene – earliest Miocene in Jylland, Denmark. Review of Palaeobotany and Palynology **159**, 166–176. *https://doi.org/10.1016/j.revpalbo.2009.12.002*

Larsson, L.M., Vajda, V. & Rasmussen, E.S. 2006: Early Miocene pollen and spores from western Jylland, Denmark – environmental and climatic implications. GFF **128**, 261–272. *https://doi.org/10.1080/11035890601283261*

Laursen, G.V. & Kristoffersen, F.N. 1999: Detailed foraminiferal biostratigraphy of Miocene formations in Denmark. Contributions to Tertiary and Quaternary Geology **36**, 73–107.

Lear, C.H., Rosenthal, Y., Coxall, H.K. & Wilson, P.A. 2004: Late Eocene to early Miocene ice sheet dynamics and the global carbon cycle. Paleoceanography and Paleoclimatology **19**, 4015. *https://doi.org/10.1029/2004PA001039*

Levy, R. *et al.* 2016: Antarctic ice sheet sensitivity to atmospheric CO_2 variations in the early to mid-Miocene. Proceedings of the National Academy of Sciences **113**, 3453–3458. *https://doi.org/10.1073/pnas.1516030113*

Lidmar-Bergström, K., Ollier, C.D. & Sulebak, J.R. 2000: Landforms and uplift history of southern Norway. Global and Planetary Change **24**, 211–231. *https://doi.org/10.1016/S0921-8181(00)00009-6*

Liu, Z., He, Y., Jiang, Y., Wang, H., Liu, W., Bohaty, S.M. & Wilson, P.A. 2018: Transient temperature asymmetry between hemispheres in the Palaeogene Atlantic Ocean. Nature Geoscience **11**, 656–660. *https://doi.org/10.1038/s41561-018-0182-9*

Mai, D.H. 1995: Tertiäre Vegetationsgeschichte Europas. Methoden und Ergebnisse. 691 pp. Gustav Fischer Verlag.

Mathiesen, F.J. 1965: Palaeobotanical investigations into some cormophytic macrofossils from the Neogene Tertiary lignites of Central Jutland. Part I: Introduction and Pteridophytes. Biologiske Skrifter **14**, 1–46. Det Kongelige Danske Videnskabernes Selskab.

Mathiesen, F.J. 1970: Palaeobotanical investigations into some cormophytic macrofossils from the Neogene Tertiary lignites of Central Jutland. Part II. Gymnosperms. Biologiske Skrifter **17**, 1–69. Det Kongelige Danske Videnskabernes Selskab.

Mathiesen, F.J. 1975: Palaeobotanical investigations into some cormophytic macrofossils from the Neogene Tertiary lignites of Central Jutland. Part III. Angiosperms. Biologiske Skrifter **20**, 1–59. Det Kongelige Danske Videnskabernes Selskab.

McCoy, J., Barrass-Barker, T., Hocking, E.P., O'Keefe, J.M.K., Riding, J.B. & Pound, M.J. 2022: Middle Miocene (Serravallian) wetland development on the northwest edge of Europe based on palynological analysis of the uppermost Brassington Formation of Derbyshire, United Kingdom. Palaeogeography, Palaeoclimatology, Palaeoecology **603**, 111180. *https://doi.org/10.1016/j.palaeo.2022.111180*

Miller, K.G., Browning, J.V., Schmelz, W.J., Kopp, R.E., Mountain, G.S. & Wright, J.D. 2020: Cenozoic sea-level and cryospheric evolution from deep-sea geochemical and continental margin records. Science Advances **6**, eaaz1346. *https://doi.org/10.1126/sciadv.aaz1346*

Miller, K.G. & Mountain, G.S. 1996: Drilling and dating New Jersey Oligocene-Miocene sequences: ice volume, Global Sea level, and Exxon records. Science **271**, 1092–1095. *https://doi.org/10.1126/science.271.5252.1092*

Miller, K.G., Wright, J.D. & Fairbanks, R.G. 1991: Unlocking the Ice House: Oligocene-Miocene oxygen isotopes, eustasy, and margin erosion. Journal of Geophysical Research: Solid Earth **96**, 6829–6848. *https://doi.org/10.1029/90JB02015*

Miller, K.G. *et al.* 2005: The phanerozoic record of global sea-level change. Science **310**, 1293–1298. *https://doi.org/10.1126/science.1116412*

Møller, L.K., Rasmussen, E.S. & Clausen, O.R. 2009: Clinoform migration patterns of a Late Miocene delta complex in the Danish Central Graben; implications for relative sea-level changes. Basin Research **21**, 704–720. *https://doi.org/10.1111/j.1365-2117.2009.00413.x*

Mörs, T. 2002: Biostratigraphy and paleoecology of continental Tertiary vertebrate faunas in the Lower Rhine Embayment (NW-Germany). Netherlands Journal of Geosciences **81**, 177–183. *https://doi.org/10.1017/S0016774600022411*

Mosbrugger, V., Utescher, T. & Dilcher, D.L. 2005: Cenozoic continental climatic evolution of Central Europe. Proceedings of the National Academy of Sciences **102**, 14964–14969. *https://doi.org/10.1073/pnas.0505267102*

Nielsen, O.B., Rasmussen, E.S. & Thyberg, B.I. 2015: Distribution of clay minerals in the Northern North Sea Basin during the Paleogene and Neogene: a result of source-area geology and sorting processes. Journal of Sedimentary Research **85**, 562–581. *https://doi.org/10.2110/jsr.2015.40*

Olivarius, M., Friis, H., Kokfelt, T.F. & Wilson, J.D. 2015: Proterozoic basement and Palaeozoic sediments in the Ringkøbing–Fyn High characterized by zircon U–Pb ages and heavy minerals from Danish onshore wells. Bulletin of the Geological Society of Denmark **63**, 29–44. *https://doi.org/10.37570/bgsd-2015-63-04*

Oskay, R.G., Bechtel, A. & Karayiğit, A.İ. 2019: Mineralogy, petrography and organic geochemistry of Miocene coal seams in the Kınık coalfield (Soma Basin-Western Turkey): insights into depositional environment and palaeovegetation. International Journal of Coal Geology **210**, 103205. *https://doi.org/10.1016/j.coal.2019.05.012*

Pälike, H., Norris, R.D., Herrle, J.O., Wilson, P.A., Coxall, H.K., Lear, C.H., Shackleton, N.J., Tripati, A.K. & Wade, B.S. 2006: The heartbeat of the Oligocene climate system. Science **314**, 1894–1898. *https://doi.org/10.1126/science.1133822*

Pearson, P.N., Foster, G.L. & Wade, B.S. 2009: Atmospheric carbon dioxide through the Eocene–Oligocene climate transition. Nature **461**, 1110–1113. *https://doi.org/10.1038/nature08447*

Petersen, H.I., Fyhn, M.B.W., Nytoft, H.P., Dybkjær, K. & Nielsen, L.H. 2022: Miocene coals in the Hanoi Trough, onshore northern Vietnam: depositional environment, vegetation, maturity, and source rock quality. International Journal of Coal Geology **253**, 103953. *https://doi.org/10.1016/j.coal.2022.103953*

Piasecki, S. 1980: Dinoflagellate cyst stratigraphy of the Miocene Hodde and Gram Formations, Denmark. Bulletin of the Geological Society of Denmark **29**, 53–76. *https://doi.org/10.37570/bgsd-1980-29-03*

Pound, M.J., Haywood, A.M., Salzmann, U., Riding, J.B., Lunt, D.J. & Hunter, S.J. 2011: A Tortonian (Late Miocene, 11.61–7.25 Ma) global vegetation reconstruction. Palaeogeography, Palaeoclimatology, Palaeoecology **300**, 29–45. *https://doi.org/10.1016/j.palaeo.2010.11.029*

Pound, M.J. & McCoy, J. 2021: Palaeoclimate reconstruction and age assessment of the Miocene flora from the Trwyn y Parc solution pipe complex of Anglesey, Wales, UK. Palynology **45**, 697–703. *https://doi.org/10.1080/01916122.2021.1916636*

Pound, M.J., Otaño, N.B.N., Romero, I.C., Lim, M., Riding, J.B. & O'Keefe, J.M.K. 2022: The fungal ecology of the Brassington Formation (Middle Miocene) of Derbyshire, United Kingdom, and a new method for palaeoclimate reconstruction. Frontiers in Ecology and Evolution **10**, 1–18. *https://doi.org/10.3389/fevo.2022.947623*

Pound, M.J. & Riding, J.B. 2016: Palaeoenvironment, palaeoclimate and age of the Brassington Formation (Miocene) of Derbyshire, UK. Journal of the Geological Society **173**, 306–319. *https://doi.org/10.1144/jgs2015-050*

Pound, M.J., Riding, J.B., Donders, T.H. & Daskova, J. 2012: The palynostratigraphy of the Brassington Formation (Upper Miocene) of the southern Pennines, central England. Palynology **36**, 26–37. *https://doi.org/10.1080/01916122.2011.643066*

Rae, J.W.B., Zhang, Y.G., Liu, X., Foster, G.L., Stoll, H.M. & Whiteford, R.D.M. 2021: Atmospheric CO_2 over the past 66 million years from Marine archives. Annual Review of Earth and Planetary Sciences **49**, 609–641. *https://doi.org/10.1146/annurev-earth-082420-063026*

Rasmussen, E.S. 1996: Sequence stratigraphic subdivison of the Oligocene and Miocene succession in South Jutland. Bulletin of the Geological Society of Denmark **43**, 143–155. *https://doi.org/10.37570/bgsd-1996-43-14*

Rasmussen, E.S. 1997: Sedimentology and sequence stratigraphy of the uppermost upper Oligocene – Miocene fluvio-deltaic system in the eastern North Sea Basin: the influence of tectonism, eustacy and climate. Unpublished doctoral thesis. University of Copenhagen.

Rasmussen, E.S. 2004: The interplay between true eustatic sea-level changes, tectonics, and climatic changes: What is the dominating factor in sequence formation of the Upper Oligocene-Miocene succession in the eastern North Sea Basin, Denmark? Global and Planetary Change **41**, 15–30. *https://doi.org/10.1016/j.gloplacha.2003.08.004*

Rasmussen, E.S. 2009a: Detailed mapping of marine erosional surfaces and the geometry of clinoforms on seismic data: a tool to identify the thickest reservoir sand. Basin Research **21**, 721–737. *https://doi.org/10.1111/j.1365-2117.2009.00422.x*

Rasmussen, E.S. 2009b: Neogene inversion of the Central Graben and Ringkøbing-Fyn High, Denmark. Tectonophysics **465**, 84–97. *https://doi.org/10.1016/j.tecto.2008.10.025*

Rasmussen, E.S. & Bruun-Petersen, J. 2010: Distribution and grain size of sand in the Miocene wave-dominated Billund delta, Denmark. Geological Survey of Denmark and Greenland Bulletin **20**, 23–26. *https://doi.org/10.34194/geusb.v20.4891*

Rasmussen, E.S., Dybkjær, K. & Piasecki, S. 2010: Lithostratigraphy of the Upper Oligocene – Miocene succession of Denmark. Geological Survey of Denmark and Greenland Bulletin **22**, 92 pp. *https://doi.org/10.34194/geusb.v22.4733*

Rasmussen, E.S., Heilmann-Clausen, C., Waagstein, R. & Eidvin, T. 2008: The Tertiary of Norden. International Union of Geological Sciences **31**, 66–72. *https://doi.org/10.18814/epiiugs/2008/v31i1/010*

Rasmussen, E.S. & Larsen, O.H. 1989: Mineralogi og geokemi af det Øvre Miocæne Gram ler. Danmarks Geologiske Undersøgelse Serie D **7**, 1–81. *https://doi.org/10.34194/seried.v7.7124*

Rasmussen, E.S., Vejbæk, O.V., Bidstrup, T., Piasecki, S. & Dybkjær, K. 2005: Late Cenozoic depositional history of the Danish North Sea Basin: implications for the petroleum systems in the Kraka, Halfdan, Siri and Nini fields. Geological Society, London, Petroleum Geology Conference Series **6**, 1347–1358. *https://doi.org/10.1144/0061347*

Rasmussen, L.B. 1966: Biostratigraphical studies on the marine younger Miocene of Denmark. Based on the molluscan faunas. Danmarks Geologiske Undersøgelse II. Række **88**, 358 pp. *https://doi.org/10.34194/raekke2.v88.6879*

Rasmussen, L.B. 1968: Molluscan Faunas and biostratigraphy of the Marine younger Miocene formations in Denmark. Part II: palaeontology. Danmarks Geologiske Undersøgelse II. Række **92**, 265 pp. *https://doi.org/10.34194/raekke2.v92.6883*

Rohling, E.J., Yu, J., Heslop, D., Foster, G.L., Opdyke, B. & Roberts, A.P. 2021: Sea level and deep-sea temperature reconstructions suggest quasi-stable states and critical transitions over the past 40 million years. Science Advances **7**, eabf5326. *https://doi.org/10.1126/sciadv.abf5326*

Sangiorgi, F., Quaijtaal, W., Donders, T.H., Schouten, S. & Louwye, S. 2021: Middle Miocene temperature and productivity evolution at a

Northeast Atlantic Shelf Site (IODP U1318, Porcupine Basin): global and regional changes. Paleoceanography and Paleoclimatology **36**, e2020PA004059. *https://doi.org/10.1029/2020PA004059*

Schellnhuber, H. J., Rahmstorf, S. & Winkelmann, R. 2016: Why the right climate target was agreed in Paris. Nature Climate Change **6**(7), 649–653. *https://doi.org/10.1038/nclimate3013*

Schuster, M., Duringer, P., Ghienne, J.-F., Vignaud, P., Mackaye, H.T., Likius, A. & Brunet, M. 2006: The age of the Sahara Desert. Science **311**, 821. *https://doi.org/10.1126/science.1120161*

Sdr. Resen. 2023: *http://www.fjendsnet.dk/00101/*

Shackleton, N.J. & Kennett, J.P. 1975: Paleotemperature history of the Cenozoic and the initiation of Antarctic glaciation: oxygen and carbon isotope analyses in DSDP sites 277, 279 and 281. Initial Report of Deep Sea Drilling Project **29**, 743. *https://doi.org/10.2973/dsdp.proc.29.117.1975*

Singh, A., Misra, B.K., Singh, B.D. & Navale, G.K.B. 1992: The Neyveli lignite deposits (Cauvery basin), India: organic composition, age and depositional pattern. International Journal of Coal Geology **21**, 45–97. *https://doi.org/10.1016/0166-5162(92)90035-U*

Śliwińska, K.K. 2019: Early Oligocene dinocysts as a tool for palaeoenvironment reconstruction and stratigraphical framework – a case study from a North Sea well. Journal of Micropalaeontology **38**, 143–176. *https://doi.org/10.5194/jm-38-143-2019*

Śliwińska, K.K., Clausen, O.R. & Heilmann-Clausen, C. 2010: A mid-Oligocene cooling (Oi-2b) reflected in the dinoflagellate record and in depositional sequence architecture. An integrated study from the eastern North Sea Basin. Marine and Petroleum Geology **27**, 1424–1430. *https://doi.org/10.1016/j.marpetgeo.2010.03.008*

Śliwińska, K.K., Dybkjær, K., Schoon, P.L., Beyer, C., King, C., Schouten, S. & Nielsen, O.B. 2014: Paleoclimatic and paleoenvironmental records of the Oligocene–Miocene transition, central Jylland, Denmark. Marine Geology **350**, 1–15. *https://doi.org/10.1016/j.margeo.2013.12.014*

Śliwińska, K.K. & Heilmann-Clausen, C. 2011: Early Oligocene cooling reflected by the dinoflagellate cyst Svalbardella cooksoniae. Palaeogeography, Palaeoclimatology, Palaeoecology **305**, 138–149. *https://doi.org/10.1016/j.palaeo.2011.02.027*

Sorgenfrei, T. 1958: Molluscan assemblages from the Marine middle Miocene of South Jutland and their environments. Vol. I. Danmarks Geologiske Undersøgelse II. Række **79**, 1–355. *https://doi.org/10.34194/raekke2.v79.6868*

Stickley, C.E. et al. 2004: Timing and nature of the deepening of the Tasmanian Gateway, Paleoceanography and Paleoclimatology **19**, PA4027. *https://doi.org/10.1029/2004PA001022*

Super, J.R., Thomas, E., Pagani, M., Huber, M., O'Brien, C. & Hull, P.M. 2018: North Atlantic temperature and pCO$_2$ coupling in the early–middle Miocene. Geology **46**, 519–522. *https://doi.org/10.1130/G40228.1*

Super, J.R., Thomas, E., Pagani, M., Huber, M., O'Brien, C. L. & Hull, P.M. 2020: Miocene evolution of North Atlantic Sea surface temperature. Paleoceanography and Paleoclimatology **35**, e2019PA003748. *https://doi.org/10.1029/2019PA003748*

The Cenozoic CO$_2$ Proxy Integration Project (CenCO$_2$PIP) Consortium. 2023: toward a Cenozoic history of atmospheric CO$_2$. Science **382**, eadi5177. *https://doi.org/10.1126/science.adi5177*

Thiede, J., Jessen, C., Knutz, P.C., Kuijpers, A., Mikkelsen, N., Nørgaard-Pedersen, N. & Spielhagen, R.F. 2010: millions of years of Greenland Ice Sheet history recorded in ocean sediments. Polarforschung **80**, 141–159.

Uhl, D. & Herrmann, M. 2010: Palaeoclimate estimates for the Late Oligocene taphoflora of Enspel (Westerwald, West Germany) based on palaeobotanical proxies. Palaeobiodiversity and Palaeoenvironments **90**, 39–47. *https://doi.org/10.1007/s12549-009-0018-0*

Uhl, D., Klotz, S., Traiser, C., Thiel, C., Utescher, T., Kowalski, E. & Dilcher, D.L. 2007: Cenozoic paleotemperatures and leaf physiognomy – a European perspective. Palaeogeography, Palaeoclimatology, Palaeoecology **248**, 24–31. *https://doi.org/10.1016/j.palaeo.2006.11.005*

Utescher, T., Ashraf, A.R., Kern, A.K. & Mosbrugger, V. 2021: Diversity patterns in microfloras recovered from Miocene brown coals of the lower Rhine Basin reveal distinct coupling of the structure of the peat-forming vegetation and continental climate variability. Geological Journal **56**, 768–785. *https://doi.org/10.1002/gj.3801*

Utescher, T., Böhme, M. & Mosbrugger, V. 2011: The Neogene of Eurasia: spatial gradients and temporal trends – the second synthesis of NECLIME. Palaeogeography, Palaeoclimatology, Palaeoecology **304**, 196–201. *https://doi.org/10.1016/j.palaeo.2011.03.012*

Utescher, T., Bondarenko, O.V. & Mosbrugger, V. 2015: The Cenozoic cooling – continental signals from the Atlantic and Pacific side of Eurasia. Earth and Planetary Science Letters **415**, 121–133. *https://doi.org/10.1016/j.epsl.2015.01.019*

Utescher, T., Gebka, M., Mosbrugger, V., Schilling, H.-D. & Ashraf, A.R. 1997: Regional palaeontological-meteorological palaeoclimate reconstruction of the Neogene Lower Rhine Embayment. Mededelingen Nederlands Instituut voor Toegepaste Geowetenschappen TNO **58**, 263–271.

Utescher, T., Mosbrugger, V. & Ashraf, A.R. 2000: Terrestrial climate evolution in Northwest Germany over the last 25 million years. Palaios **15**, 430–449. *https://doi.org/10.1669/0883-1351(2000)015<0430:TCEING>2.0.CO;2*

Utescher, T., Mosbrugger, V. & Ashraf, A.R. 2002: Facies and paleogeography of the Tertiary of the Lower Rhine Basin – sedimentary versus climatic control. Netherlands Journal of Geosciences **81**, 185–191. *https://doi.org/10.1017/S0016774600022423*

Utescher, T. et al. 2014: The coexistence approach – theoretical background and practical considerations of using plant fossils for climate quantification. Palaeogeography, Palaeoclimatology, Palaeoecology **410**, 58–73. *https://doi.org/10.1016/j.palaeo.2014.05.031*

Wade, B.S. & Pälike, H. 2004: Oligocene climate dynamics. Paleoceanography and Paleoclimatology **19**, 1–16. *https://doi.org/10.1029/2004PA001042*

Wagner, P. & Koch, B.E. 1974: Fossil roots of Sequoia type from two localities of the Miocene delta deposits. Bulletin of the Geological Society of Denmark **23**, 134–158.

Weibel, R. 1996: Petrified wood from an unconsolidated sediment, Voervadsbro, Denmark. Sedimentary Geology **101**, 31–41. *https://doi.org/10.1016/0037-0738(95)00013-5*

Westerhold, T. et al. 2020: An astronomically dated record of Earth's climate and its predictability over the last 66 million years. Science **369**, 1383–1387. *https://doi.org/10.1126/science.aba6853*

Widera, M. 2016: An overview of lithotype associations of Miocene lignite seams exploited in Poland. Geologos **22**, 213–225. *https://doi.org/10.1515/logos-2016-0022*

Worobiec, E., Widera, M., Worobiec, G. & Kurdziel, B. 2021: Middle Miocene palynoflora from the Adamów lignite deposit, central Poland. Palynology **45**, 59–71. *https://doi.org/10.1080/01916122.2019.1697388*

Zachos, J., Pagani, M., Sloan, L., Thomas, E. & Billups, K. 2001: Trends, rhythms, and aberrations in global climate 65 Ma to present. Science **292**, 686–693. *https://doi.org/10.1126/science.1059412*

Zetter, R. 1997: Palynological investigations from the early Miocene lignite opencast mine Oberdorf (N Voitsberg, Styria, Austria). Jahrbuch der Geologischen Bundesanstalt Wien **140**, 461–468.

Ziegler, P.A. 1990: Geological atlas of Western and Central Europe, 2nd edition, 239 pp. The Hague: Shell Internationale Petroleum Maatschappij, B.V.